

Alkylated organic cages: from porous crystals to neat liquids

Nicola Giri, Christine E. Davidson, Gavin Melaugh, Mario del Popolo, James T. A. Jones, Tom Hasell, Andrew I. Cooper, Peter N. Horton, Michael B. Hursthouse, Stuart L. James

Supplementary Information

Contents

| | page |
|--|------|
| Synthetic and other experimental details | 4 |
| Figure S1. $^1\text{H-NMR}$ (300 MHz, CDCl_3) of cage 6 . | 19 |
| Figure S2. $^{13}\text{C-NMR}$ (125 MHz, CDCl_3) of cage 6 . | 19 |
| Figure S3. $^1\text{H-NMR}$ (300 MHz, CDCl_3) of cage 7 . | 20 |
| Figure S4. $^{13}\text{C-NMR}$ (75 MHz, CDCl_3) of cage 7 . | 20 |
| Figure S5. $^1\text{H-NMR}$ (300 MHz, CDCl_3) of cage 8 . | 21 |
| Figure S6. $^{13}\text{C-NMR}$ (125 MHz, CDCl_3) of cage 8 . | 21 |
| Figure S7. $^1\text{H-NMR}$ (300 MHz, CDCl_3) of cage 9 . | 22 |
| Figure S8. $^{13}\text{C-NMR}$ (125 MHz, CDCl_3) of the octyl cage (8). | 22 |
| Figure S9. $^{13}\text{C-NMR}$ (125 MHz, CDCl_3) of cage 9 . | 23 |
| Figure S10. DSC trace of the pentyl cage (7) | 23 |
| Figure S11. DSC trace of the isohexyl cage (8) | 24 |
| Figure S12. Visual melting of the hexyl cage (6). | 24 |
| Figure S13. Visual melting of the pentyl cage (7). | 25 |
| Figure S14. Visual melting of the isohexyl cage (8). | 25 |
| Figure S15. The packing motif in the crystal structure of isohexyl cage 8 (H-atoms and solvent molecules omitted for clarity). | 26 |
| Figure S16. Molecular structure of <i>n</i> -pentyl cage 7 in the crystal showing the disorder in the chains (solvent molecules omitted for clarity). | 27 |
| Figure S17. View of the crystal structure of <i>n</i> -pentyl cage 7 along the crystallographic <i>a</i> axis (H-atoms and solvent molecules omitted for clarity). | 28 |
| Figure S18. View of the crystal structure of <i>n</i> -pentyl cage 7 along the | 29 |

| | |
|---|----|
| crystallographic <i>b</i> axis (H-atoms and solvent molecules omitted for clarity). | |
| Figure S19. View of the crystal structure of <i>n</i> -pentyl cage 7 along the crystallographic <i>c</i> axis (H-atoms and solvent molecules omitted for clarity). | 30 |
| Figure S20. View of the crystal structure of <i>n</i> -pentyl cage 7 between the crystallographic axes (H-atoms and solvent molecules omitted for clarity). | 31 |
| Figure S21. Amplitude sweep for the cage 9 showing Elastic modulus G' (Pa), Viscous modulus G'' (Pa) and phase angle δ ($^{\circ}$) with increasing strain γ (%). 50 $^{\circ}$ C, 1Hz. Load 1 (circles) and Load 2 (triangles). | 32 |
| Figure S22. Amplitude sweep for cage 9 showing Elastic modulus G' (Pa), Viscous modulus G'' (Pa) and phase angle δ ($^{\circ}$) with increasing strain γ (%). 100 $^{\circ}$ C, 1Hz. | 33 |
| Figure S23. Frequency sweep for cage 9 showing Elastic modulus G' (Pa), Viscous modulus G'' (Pa) and phase angle δ ($^{\circ}$) across a range of frequencies at 50 $^{\circ}$ C. Load 1 (triangles) and Load 2 (circles) | 34 |
| Figure S24. Frequency sweep for cage 9 showing Complex viscosity η^* (Pa.s) across a range of frequencies at 25 $^{\circ}$ C. Load 1 (triangles) and Load 2 (circles). | 35 |
| Figure S25. Frequency sweep for cage 9 showing elastic modulus G' (Pa), viscous modulus G'' (Pa), complex viscosity η^* (Pa.s) and phase angle δ ($^{\circ}$) across a range of frequencies at 100 $^{\circ}$ C. | 36 |
| Figure S26. Frequency sweep for cage 9 showing elastic modulus G' (Pa), viscous modulus G'' (Pa), complex viscosity η^* (Pa.s) and phase angle δ ($^{\circ}$) across a range of frequencies at 60 $^{\circ}$ C. | 37 |
| Figure S27. Temperature sweep of cage 9 between 40 $^{\circ}$ C and 90 $^{\circ}$ C, at 1Hz and 2 $^{\circ}$ C/min showing showing Elastic modulus G' (Pa), viscous modulus G'' (Pa) and phase angle δ ($^{\circ}$).Load 1 (triangles), Load 1.2 (squares) and Load 2 (circles). | 38 |
| Figure S28. Temperature sweep of cage 9 between 40 $^{\circ}$ C and 90 $^{\circ}$ C, at 0.1Hz and 2 $^{\circ}$ C/min showing elastic modulus G' (Pa), viscous modulus G'' (Pa) and phase angle δ ($^{\circ}$). Load 1.1(0.1Hz). | 39 |
| Figure S29. Photograph of a fibre of cage 9 drawn out from the melt. | 40 |
| Figure S30. a) TGA of the isohexyl cage 8 , b) TGA of the octyl cage 9 . | 40 |

| | |
|---|----|
| Figure S31. PXRD Le Bail profile fit of the desolvated isohexyl cage 8 measured after gas sorption analysis. (space group <i>I</i> 23, $a = 19.2015(6) \text{ \AA}$, $V = 7079 (6) \text{ \AA}^3$, Agreement factors, $R_{\text{wp}} = 6.36$, $R_{\text{exp}} = 3.55$, $R_p = 4.50$, $GoF = 1.79$). | 41 |
| Figure S32. N ₂ adsorption/ desorption isotherm recorded at 77 K on the isohexyl Cage 8 . Inset is the NL-DFT pore size distribution plot calculated using the adsorption branch of the isotherm. | 42 |
| Figure S33. Calculated N ₂ absorption isotherm for isohexyl cage 8 , with a snapshot of the fully saturated system (inset). | 42 |
| Figure S34. Powder X-ray diffraction pattern for octyl cage 9 . | 43 |

Experimental

NMR. ^1H , ^{13}C NMR spectra were all recorded on Bruker AM 300 MHz or AM 500 MHz referenced to the residual ^1H or ^{13}C containing solvent. Chemical shifts (δ) are given in parts per million (ppm) and coupling constants are given in Hertz.

Elemental analysis. Elemental analysis were determined by the Analytical Service Department of the School of Chemistry (ASEP) using a Perkin-Elmer 2400 CHN microanalyser.

Mass Spectrometry. Mass spectrometry was performed using a Micromass MALDI-TOF mass spectrometer using CHCA as a matrix. Calibration in the mass range was performed using PEG.

Scanning Electron Microscopy. High resolution imaging of the crystal morphology was achieved using a Hitachi S-4800 cold Field Emission Scanning Electron Microscope (FE-SEM). The dry samples were prepared on 15 mm Hitachi M4 aluminium stubs using either silver dag or an adhesive high purity carbon tab. The samples were then coated with a 2 nm layer of gold using an Emitech K550X automated sputter coater. The FE-SEM measurement scale bar was calibrated using certified SIRA calibration standards. Imaging was conducted at a working distance of 8 mm and a working voltage of 3 kV using a mix of upper and lower secondary electron detectors.

Thermogravimetric Analysis. TGA analysis was carried out using a Q5000IR analyzer (TA instruments) with an automated vertical overhead thermobalance. The samples were heated at the rate of 5 $^{\circ}\text{C}/\text{min}$.

Differential Scanning Calorimetry. DSC analysis was carried out using a DSC Q2000 at a heating/cooling rate of 10 $^{\circ}\text{C}/\text{min}$.

Powder X-ray Diffraction. Powder X-ray diffraction data were collected on a Panalytical X'pert pro multi-purpose diffractometer (MPD) in reflection Bragg-Brentano geometry operating with a Cu anode at 40 kV 40 mA. Samples were mounted as loose powder onto a silicon zero background holder. PXRD patterns were collected in 16 1 hour scans with a step size of 0.00657 degrees 2 theta and scan time of 115 s/step over 2 – 50 deg 2 theta on a sample stage rotating at 2s/rotation. The incident X-ray beam was conditioned with 0.04 rad Soller slits, automatic divergence slit (5 mm), mask (5 mm) and anti-scatter slit of 1 deg. The diffracted beam passed through an automatic antiscatter slit (5 mm), 0.04 rad Soller slits and Ni filter before processing by the PIXcel detector operating in scanning mode.

Visual Melting. The visual melting pictures were recorded using an hot-stage Olympus BX 50 Phase Pol Darkfield Microscope.

Gas Sorption Analysis. All samples were tested with gas of the following purities: hydrogen (99.9995% - BOC gases). Surface areas and pore size distributions were measured by nitrogen adsorption and desorption at 77.3 K using a Micromeritics ASAP 2020 volumetric adsorption analyzer. Samples were degassed at 80 °C for 15 h under vacuum (10⁻⁵ bar) before analysis. Isotherms for hydrogen were measured at 77.3 K (liquid N₂). All data points were measured to 98% equilibration and fitted to a linear driving force model using the IGASWIN software (v1.03.148).

Single Crystal X-ray Diffraction The crystallographic data collection of compounds **7** and **8** were performed using a Nonius Kappa CCD diffractometer with Mo Ka radiation ($\lambda = 0.71073\text{\AA}$) controlled by the Collect¹ software package. The data were processed using Denzo² and semi-empirical absorption corrections were applied using SADABS³. The structures were solved by direct methods and refined by full-matrix least-square procedures on F^2 using SHELXS-97⁴ and SHELXL-97⁴ 15 respectively. All non-hydrogen atoms were refined anisotropically, with all hydrogen atoms placed geometrically using standard riding models. The temperatures used were due to observed crystal cracking at 150K and 120K respectively. Both compounds crystallise in chiral space groups, however it was not possible to accurately determine the chirality using the Flack parameter and thus all Friedel pairs were merged. The given chirality is based on the known reactants and the reactions used. For compound **7**, it was not possible to satisfactorily model the included solvent and thus the data were treated with the SQUEEZE⁵ routine in PLATON⁶.

Compound **8** refined as a merohedral twin (matrix: 0 -1 0 -1 0 0 0 0 -1) at 34.8%

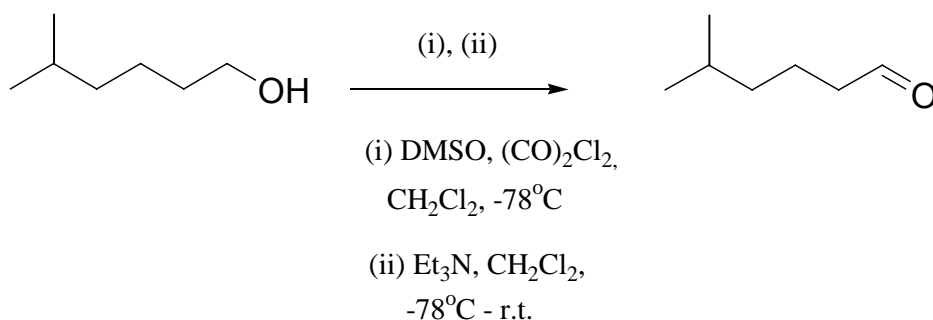
Sorption modelling In order to investigate the distribution of N₂ molecules in the crystal phase of the isohexyl cage (**8**), the gas absorption isotherm was computed by Grand Canonical (GC) Monte Carlo simulations at 77 K and in the range 10⁻³ – 0.5 atm. The simulation cell consisted of eight crystal unit cells (16 cage molecules in total) under periodic boundary conditions. At each pressure, the cell parameters and the initial configuration of the solid were set to those of the experimental X-ray structure. During the Markov chain displacements of individual atoms were

attempted with a probability of 0.3, rigid rotations of N₂ molecules with a probability of 0.2 and insertion/deletion of N₂ molecules with a probability of 0.5. A typical simulation consisted of 10⁷ trial moves. It is important to mention that even when all the atoms in the system were allowed to move, only small fluctuations in the atomic positions were observed during the course of a simulation. This is expected given the close packing of the particles in the crystal and the low temperature of the sample. The N₂ molecules exhibited little rotational freedom, except for those located at the centre of a cage that explored different orientations due to the insertion/deletion moves.

Cage molecules were modelled with the OPLS force-field,⁷ which is of standard use in simulation of organic molecules. Non-bonded interactions were described by Lennard-Jones potentials and no partial charges were included in any of the atoms. N₂ molecules were modelled by two Lennard-Jones particles ($\sigma = 3.329 \text{ \AA}$, $\epsilon/k_B = 37.3 \text{ K}$) connected through a rigid bond ($r_{eq} = 1.089 \text{ \AA}$).⁸ Cross-species interaction parameters were calculated through the Lorentz–Berthelot combining rules: $\sigma_{ij} = (\sigma_i + \sigma_j)/2$, $\epsilon_{ij} = (\epsilon_i \epsilon_j)^{1/2}$

Materials. 1,3,5-Triformylbenzene was prepared by standard literature procedures^{9,10} or purchased from Manchester Organics. All other chemicals were purchased from Sigma-Aldrich and used as received.

5-Methylhexanal

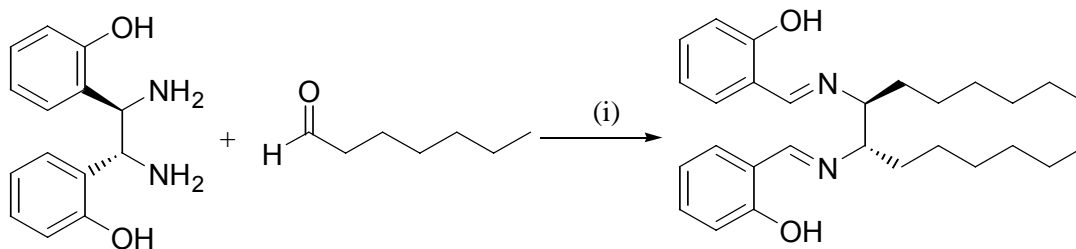


DMSO (1.540 ml, 21.72 mmol) was dissolved in 35 ml of dry CH_2Cl_2 under nitrogen, cooled to -78°C and treated with oxalyl chloride (1.870 ml, 11.03 mmol). After stirring at this temperature for 15 min., 5-Methylhexanol (1.200 ml, 8.62 mmol) in 10 ml of dry CH_2Cl_2 , was added dropwise. After stirring for 20 min. at -78°C , triethylamine was added and the mixture stirred at the same temperature for further 15 min. and then allowed to room temperature. Ammonium Chloride saturated solution was used to quench the reaction and the mixture was extracted with diethyl ether. The organic phase was then washed with brine and dried over sodium sulfate. The residue was purified by column chromatography (pentane/diethyl ether = 9/1) to afford a colourless oil (0.750 g, yield 76%).

$^1\text{H-NMR}$ (300 MHz, CDCl_3): δ 9.76 (s, 1H), 2.40 (t, 2H, $^3J_{\text{HH}} = 6$ Hz), 1.67-1.51 (m, 3H), 1.23-1.20 (m, 2H), 0.88 (d, 6H, $^3J_{\text{HH}} = 6$ Hz).

$^{13}\text{C-NMR}$ (75 MHz, CDCl_3): δ 203.1, 44.3, 38.5, 28.0, 22.6, 20.1.

(S,S)-N,N'-bis(salicylidene)-1,2-hexyl-1,2-diaminoethane



(i) Toluene, Dean-Stark apparatus

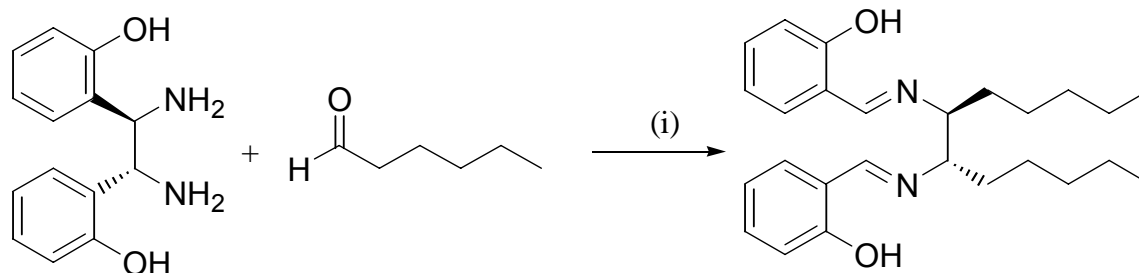
Heptanal (2.86 ml, 20.5 mmol) was added to a solution of (*R,R*)-1,2-bis(2-hydroxyphenyl)-1,2-diaminoethane (2.0g, 8.2 mmol) in toluene (25ml) at ambient temperature. The resulting solution was refluxed overnight with a Dean-Stark trap. After removal of the solvent under reduced pressure, the resulting viscous yellow oil was purified by column chromatography (eluent: DCM 100%). 2.580 g of a yellow oil was obtained (yield 72 %).

$^1\text{H-NMR}$ (300 MHz, CDCl_3): δ 13.42 (br s, 2H), 8.25 (s, 2H), 7.31-7.25 (m, 2H), 7.20 (dd, $^3J_{\text{HH}}=9$ Hz, $^4J_{\text{HH}}=3$ Hz, 2H), 6.96 (d, $J=9$ Hz, 2H); 6.84 (t, $J=9$ Hz, 2H), 3.29-3.26 (m, 2H), 1.67 (m, 4H), 1.25 (m, 16H), 0.87 (t, $^3J_{\text{HH}}=6$ Hz, 6H).

$^{13}\text{C-NMR}$ (75 MHz, CDCl_3): δ 165.0, 161.5, 132.3, 131.5, 118.7, 118.6, 117.2, 73.9, 32.7, 31.9, 29.3, 26.4, 22.7, 14.2.

MS (ES^+) 437 ($[\text{M}+\text{H}]^+$).

(S,S)-N,N'-bis(salicylidene)-1,2-pentyl -1,2-diaminoethane



(i) Toluene, Dean-Stark apparatus

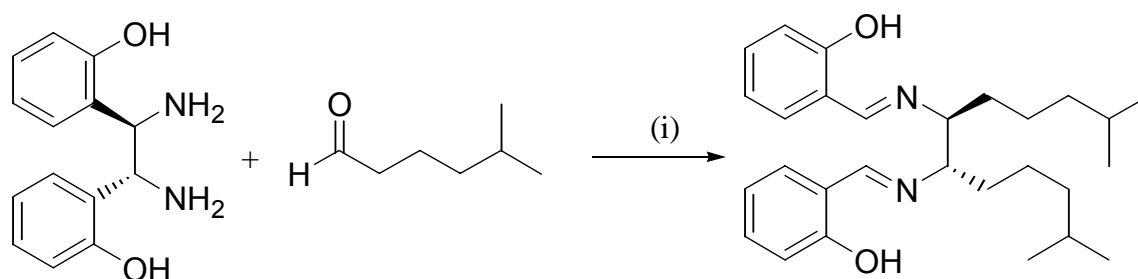
Hexanal (1.23 ml, 10.25 mmol) was added to a solution of (R,R)-1,2-bis(2-hydroxyphenyl)-1,2-diaminoethane (1.0 g, 4.1 mmol) in toluene (25 ml) at ambient temperature. The resulting solution was refluxed overnight with a Dean-Stark trap. After removal of the solvent under reduced pressure, the resulting viscous yellow oil was purified by precipitation using methanol to give a yellow solid (1.04 g, yield 62 %).

$^1\text{H-NMR}$ (300 MHz, CDCl_3): δ 13.48 (br s, 2H), 8.25 (s, 2H), 7.28(ddd, $^3J_{\text{HH}} = 9\text{Hz}$, $^4J_{\text{HH}} = 1\text{ Hz}$ 2H), 7.22 (dd, $^3J_{\text{HH}} = 9\text{ Hz}$, $^4J_{\text{HH}} = 1\text{ Hz}$, 2H), 6.97 (d, $^3J_{\text{HH}} = 6\text{ Hz}$, 2H), 6.84 (ddd, $^3J_{\text{HH}} = 6\text{ Hz}$, $^4J_{\text{HH}} = 1\text{ Hz}$, 2H), 3.29-3.22(m, 2H), 1.66 (m, 4H), 1.26 (m, 12H), 0.85 (t, $^3J_{\text{HH}} = 6\text{ Hz}$, 6H).

$^{13}\text{C-NMR}$ (75 MHz, CDCl_3): δ 165.3, 161.7, 132.6, 131.8, 118.9, 118.9, 117.5, 74.1, 32.9, 32.0, 26.3, 22.9, 14.4.

MS (ES^+) 409 ($[\text{M}+\text{H}]^+$).

(S,S)-N,N'-bis(salicylidene)-1,2-isoheptyl-1,2-diaminoethane



(i) Toluene, Dean-Stark apparatus

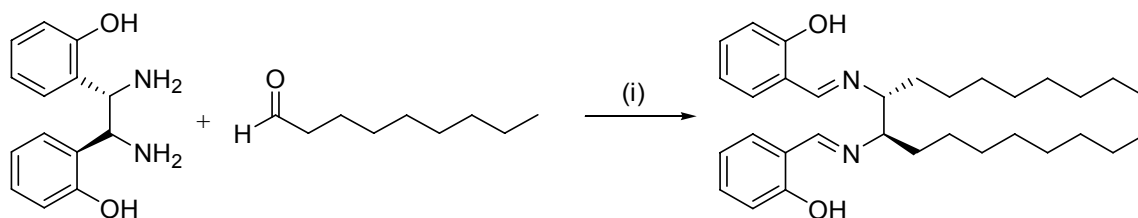
5-methyl-hexanal (1.500 g, 13.15 mmol) was added to a solution of (R,R)-1,2-bis(2-hydroxyphenyl)-1,2-diaminoethane (1.280 g, 5.26 mmol) in toluene (20 ml) at ambient temperature. The resulting solution was refluxed overnight with a Dean-Stark trap. After removal of the solvent under reduced pressure, the resulting viscous yellow oil was purified by column chromatography (DCM) (1.730 g, yield 76%).

$^1\text{H-NMR}$ (300 MHz, CDCl_3): δ 13.47 (s, 2H), 8.26 (s, 2H), 7.31-7.26 (m, 2H), 7.21 (dd, $^3J_{\text{HH}} = 9$ Hz, $^4J_{\text{HH}} = 1$ Hz, 2H), 6.97 (d, $^3J_{\text{HH}} = 6$ Hz, 2H), 6.84 (ddd, $^3J_{\text{HH}} = 6$ Hz, $^4J_{\text{HH}} = 1$ Hz, 2H), 3.31-3.25 (m, 2H), 1.66 -1.42 (m, 6H), 1.35-1.11 (m, 8H), 0.83 (d, $^3J_{\text{HH}} = 6$ Hz, 6H), 0.82 (d, $^3J_{\text{HH}} = 6$ Hz, 6H).

$^{13}\text{C-NMR}$ (75 MHz, CDCl_3): δ 165.3, 161.7, 132.6, 131.7, 118.9, 118.9, 117.5, 74.1, 39.1, 33.2, 28.2, 24.4, 23.1, 22.9.

MS (ES^+) 437 ($[\text{M}+\text{H}]^+$).

(*S,S*)-*N,N*-bis(salicylidene)-1,2-octyl-1,2-diaminoethane



(i) Toluene, Dean-Stark apparatus

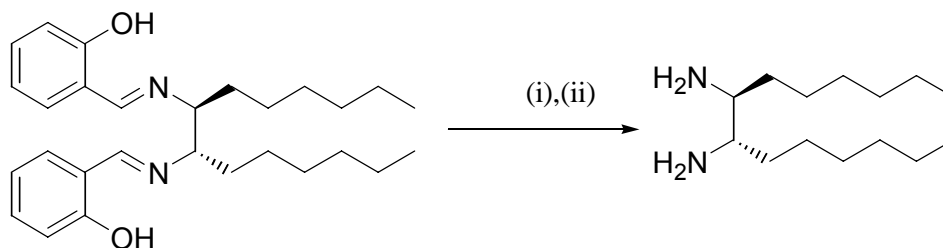
Nonanal (3.52 ml, 20.5 mmol) was added to a solution of (*S,S*)-1,2-bis(2-hydroxyphenyl)-1,2-diaminoethane (2.0 g, 8.2 mmol) in toluene (25 ml) at ambient temperature. The resulting solution was refluxed for overnight with a Dean-Stark trap. After removal of the solvent under reduced pressure, the resulting viscous yellow oil was purified by column chromatography (eluent: DCM 100%). 2.2 g of a yellow oil was obtained (yield 55 %).

$^1\text{H-NMR}$ (300 MHz, CDCl_3): δ 13.48 (br s, 2H), 8.25 (s, 2H), 7.28 (ddd, $^3J_{\text{HH}} = 6\text{ Hz}$, $^4J_{\text{HH}} = 2\text{ Hz}$, 2H), 7.20 (dd, $^3J_{\text{HH}} = 6\text{ Hz}$, $^4J_{\text{HH}} = 2\text{ Hz}$, 2H), 6.97 (d, $^3J_{\text{HH}} = 8\text{ Hz}$, 2H); 6.83 (ddd, $^3J_{\text{HH}} = 8\text{ Hz}$, $^4J_{\text{HH}} = 1\text{ Hz}$, 2H), 3.28-3.24 (m, 2H), 1.66-1.58 (m, 4H), 1.22 (m, 24H), 0.85 (t, $^3J_{\text{HH}} = 9\text{ Hz}$, 6H).

$^{13}\text{C-NMR}$ (75 MHz, CDCl_3): δ 165.2, 161.7, 132.6, 131.8, 118.9, 118.8, 117.5, 74.1, 53.8, 33.0, 32.2, 29.7, 26.6, 23.0, 14.5.

MS (ES^+) 493 ($[\text{M}+\text{H}]^+$).

(*S,S*)-1,2-hexyl-1,2-diaminoethane



(i) THF/HCl 37% solution, r.t., overnight
(ii) NaOH 1M

To a clear, yellow solution of (*S,S*)-*N,N*-bis(salicylidene)-1,2-hexyl-1,2-diaminoethane (5.7 mmol) in 25 mL of THF was added a mixture of 1.7 mL of 37% HCl solution and 25 ml of THF.

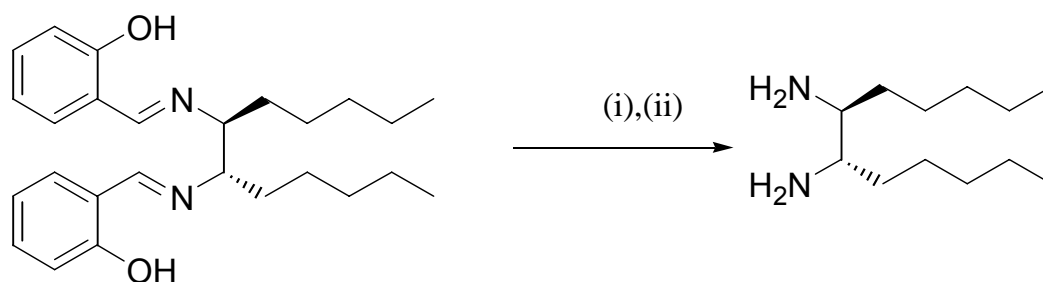
After stirring the mixture at r.t. for 24 hrs, the mixture was diluted with 100 ml of diethyl ether and extracted three times with 30 ml of water. The water phase was basified with NaOH 1.0 M, extracted three times with 50 ml of DCM and dried over dry Na₂SO₄. 1.46 g of diamine (yield 86%) was obtained as a red liquid and used without further purification.

¹H-NMR (300 MHz, CDCl₃): δ 2.52 (bs, 2H, NC*H), 1.40-1.41 (m, 4H), 1.28 (m, 16H), 1.13 (bs, 4H), 0.88 (t, ³J_{HH} = 6 Hz, 6H).

¹³C-NMR (75 MHz, CDCl₃): 55.4, 35.1, 32.0, 29.6, 26.7, 22.8, 14.2

MS (ES⁺) 229 ([M+H]⁺).

(S,S)-1,2-pentyl-1,2-diaminoethane



- (i) THF/HCl 37% solution, r.t., overnight
(ii) NaOH 1M

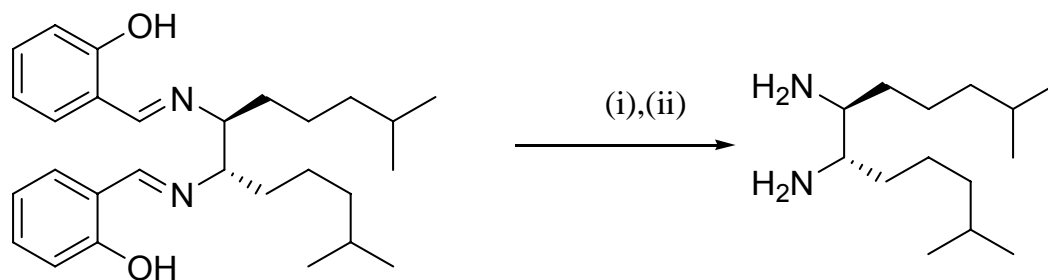
To a clear, yellow solution of (S,S)-N,N'-bis(salicylidene)-1,2-pentyl-1,2-diaminoethane (2.6 mmol) in 12 mL of THF was added a mixture of 0.78 mL of 37% HCl solution and 12 ml of THF. After stirring the mixture at r.t. for 24 hrs, the mixture was diluted with 50 ml of diethyl ether and extracted three times with 15ml of water. The water phase was basified with NaOH 1.0 M, extracted three times with 30 ml of DCM and dried over dry Na₂SO₄. 0.32g of diamine (yield 60%) was obtained as a red liquid and used without further purification.

¹H-NMR (300 MHz, CDCl₃): δ 2.53 (bs, 2H), 1.42-1.30 (m, 16H), 1.10 (bs, 4H), 0.90 (t, ³J_{HH} = 7 Hz, 6H).

¹³C-NMR (75 MHz, CDCl₃): δ 55.7, 35.4, 32.4, 26.8, 23.1, 14.5

MS (ES⁺) 201 ([M+H]⁺).

(S,S)-1,2-isoheptyl-1,2-diaminoethane



- (i) THF/HCl 37% solution, r.t., overnight
(ii) NaOH 1M

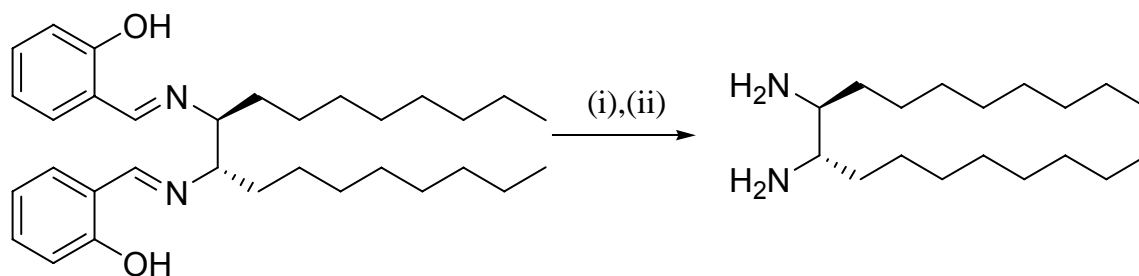
To a clear, yellow solution of (S,S)-N,N'-bis(salicylidene)-1,2-isoheptyl-1,2-diaminoethane (1.730 g, 3.98 mmol) in 15 mL of THF was added a mixture of 1.23 mL of 37% HCl solution and 15 ml of THF. After stirring the mixture at r.t. for 24 hrs, the mixture was diluted with 50 ml of diethyl ether and extracted three times with 15 ml of water. The water phase was basified with NaOH 1.0 M, extracted three times with 30 ml of DCM and dried over dry Na₂SO₄. 0.800 g of diamine (yield 88%) was obtained as a red liquid and used without further purification.

¹H-NMR (300 MHz, CDCl₃): δ 2.54 (d, 2H, ³J_{HH} = 6 Hz), 1.56-1.17 (m, 18H), 0.87 (t, ³J_{HH} = 9 Hz, 6H).

¹³C-NMR (75 MHz, CDCl₃): δ 55.5, 39.3, 35.3, 28.1, 24.5, 22.8, 22.7.

MS (ES⁺) 229 ([M+H]⁺).

(S,S)-1,2-octyl-1,2-diaminoethane



- (i) THF/HCl 37% solution, r.t., overnight
(ii) NaOH 1M

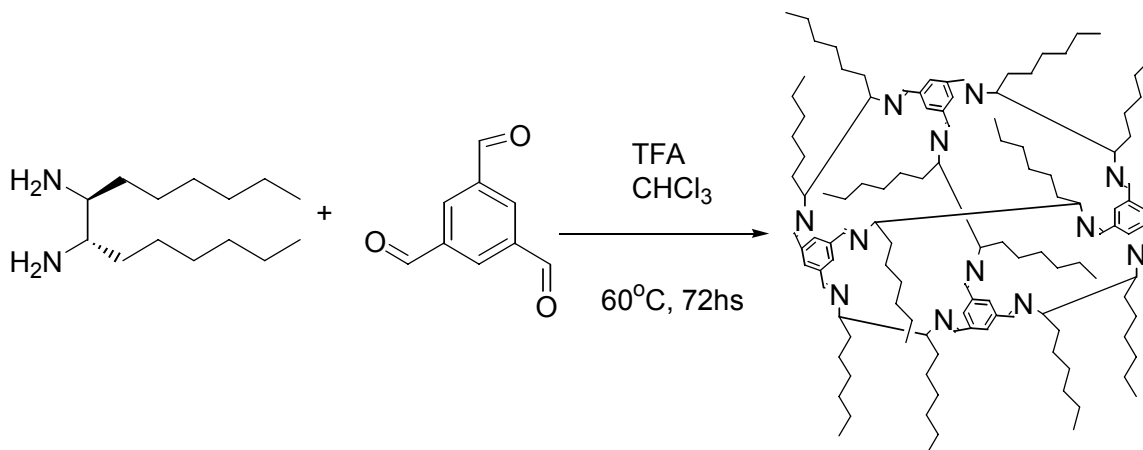
To a clear, yellow solution of *(R,R)*-*N,N'*-bis(salicylidene)-1,2-octyl-1,2-diaminoethane (2.2 g, 4.5 mmol) in 20 mL of THF was added a mixture of 1.35 mL of 37% HCl solution and 20 ml of THF. After stirring the mixture at r.t. for 24 hrs, the mixture was diluted with 50 ml of diethyl ether and extracted three times with 15ml of water. The water phase was basified with NaOH 1.0 M, extracted three times with 30 ml of DCM and dried over dry Na₂SO₄. 0.990 g of diamine (yield 77%) was obtained as a red liquid and used without further purification.

¹H-NMR (300 MHz, CDCl₃): δ 2.54 (bs, 2H), 1.44-1.27 (m, 28H), 1.13 (bs, 4H), 0.88 (t, ³J_{HH} = 6 Hz, 6H).

¹³C-NMR (75 MHz, CDCl₃): δ 55.6, 35.5, 32.3, 30.3, 30.0, 29.7, 27.0, 23.1, 14.5.

MS (ES⁺) 285 ([M+H]⁺).

Hexyl cage (6)



(S,S)-1,2-hexyl-1,2-diaminoethane (0.497g, 2.2 mmol) was dissolved in 10 ml of CHCl₃ and TFB (0.196g, 1.2 mmol) dissolved in 7 ml CHCl₃ and trifluoroacetic acid (0.035 ml, 0.45 mmol) were added. After heating the reaction mixture at 60°C for 72 hrs, the solvent was removed under reduced pressure and the crude purified by column chromatography (eluent: benzene/ethyl acetate 99/1). (160 mg, yield 30%).

m.p. 126°C

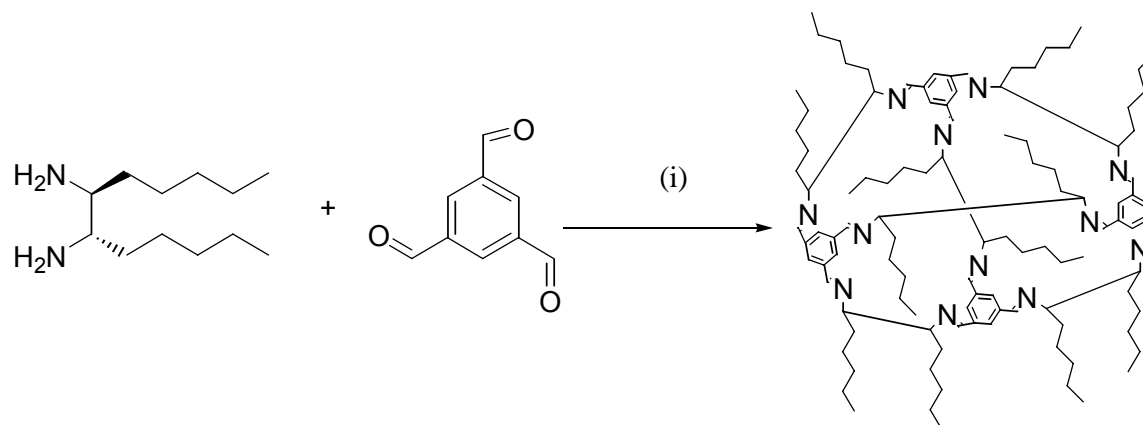
¹H-NMR (300 MHz, CDCl₃): δ 8.06 (s, 12H), 7.88 (s, 12H), 3.33 (d, ³J_{HH} = 6 Hz, 12H), 1.79-1.65 (m, 24 H), 1.24-1.09 (m, 96 H), 0.85 (t, ³J_{HH} = 6 Hz, 36 H).

¹³C-NMR (125 MHz, CDCl₃): δ 159.7, 137.0, 130.0, 75.8, 32.2, 29.6, 26.8, 22.1, 14.5.

MS (MALDI-TOF⁺) 1804 ([M+H]⁺), 1826 ([M+Na]⁺), 1842 ([M+K]⁺).

CHN analysis for C₁₂₀H₁₉₂N₁₂: C 79.94, H 10.73, N 9.32; found C 78.44, H 10.26, N 9.12.

Pentyl cage (7)



(i) TFA, CHCl_3 , 65°C , 72hrs

(S,S)-1,2-pentyl-1,2-diaminoethane (0.145g, 0.73 mmol) was dissolved in 3.3 ml of CHCl_3 and TFB (0.06g, 0.40 mmol) dissolved in 2.3 ml CHCl_3 and trifluoroacetic acid (0.01 ml, 0.13 mmol) were added. After heating the reaction mixture at 60°C for 72 hrs, the solvent was removed under reduced pressure and the crude purified by precipitation from acetone. Crystals were grown diffusing acetone in a solution of the pentyl cage in DCM (0.063 mg, yield 63%).

M.p. = 156°C

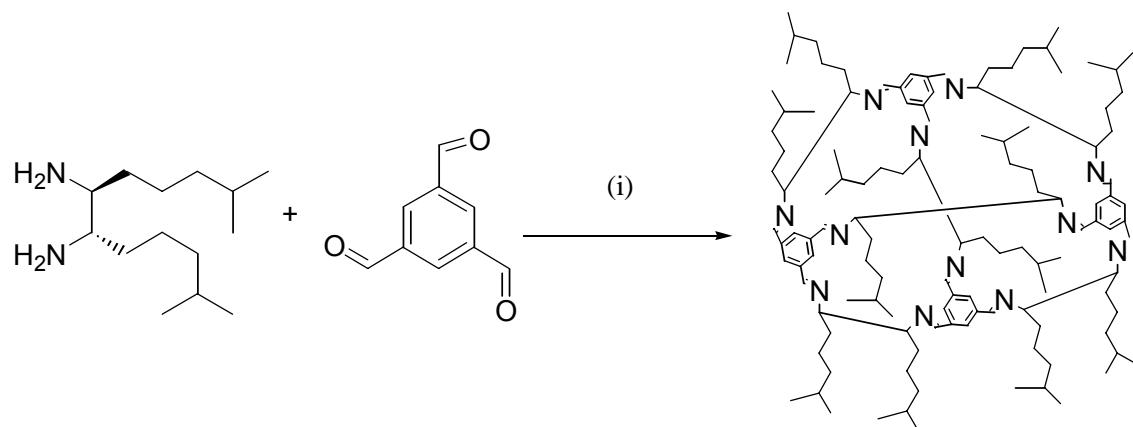
$^1\text{H-NMR}$ (300 MHz, CDCl_3): δ 8.06 (s, 12H), 7.87 (s, 12H), 3.33 (d, $^3J_{\text{HH}} = 8$ Hz, 12H), 1.78-1.65 (m, 24 H), 1.25-1.08 (m, 72 H), 0.84 (t, $^3J_{\text{HH}} = 6$ Hz, 36 H).

$^{13}\text{C-NMR}$ (125 MHz, CDCl_3): δ 159.7, 137.0, 129.9, 75.8, 32.2, 26.5, 23.0, 14.5.

MS (MALDI-TOF) 1635 ($[\text{M}+\text{H}]^+$) 1658 ($[\text{M}+\text{Na}]^+$)

CHN analysis for $\text{C}_{108}\text{H}_{168}\text{N}_{12}$: C 79.36, H 10.36, N 9.28; found C 78.24, H 9.75, N 10.56.

Isohexyl cage (8)



(i) TFA, CHCl₃, 65°C, 72hrs

(S,S)-1,2-isohexyl-1,2-diaminoethane (0.740 g, 3.24 mmol) was dissolved in 5 ml of CHCl₃ and TFB (0.262 g, 1.62 mmol) dissolved in 5 ml CHCl₃ and trifluoroacetic acid (0.046 ml, 0.61 mmol) were added. After heating the reaction mixture at 65°C for 72 hrs, the solvent was removed under reduced pressure and the crude purified by precipitation from acetone. Crystals were grown diffusing acetone in a solution of the isohexyl cage in chloroform (0.140 mg, yield 35%).

M.p. = 198°C

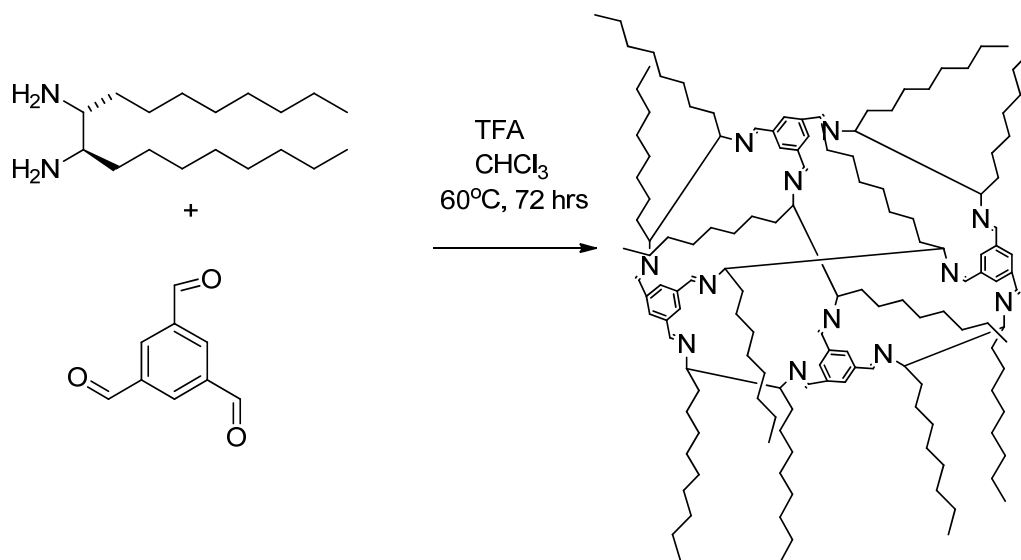
¹H-NMR (300 MHz, CDCl₃): δ 8.07 (s, 12H), 7.88 (s, 12H), 3.34 (d, ³J_{HH} = 6 Hz, 12H), 1.77-1.51 (m, 24H), 1.47-1.42 (m, 12H), 1.16-1.14 (m, 48H), 0.81, (d, ³J_{HH} = 6 Hz, 36H), 0.80 (d, ³J_{HH} = 6 Hz, 36H),

¹³C-NMR (125 MHz, CDCl₃): δ 159.7, 137.0, 130.0, 75.7, 39.2, 32.5, 28.2, 24.4, 23.2, 22.8

MS (MALDI-TOF) 1803.5 ([M+H]⁺).

CHN analysis for C₁₂₀H₁₉₂N₁₂: C 79.94, H 10.73, N 9.32; found C 79.62, H 11.17, N 9.29.

Octyl cage (9)



(*R,R*)-1,2-octyl-1,2-diaminoethane (0.99 g, 3.47 mmol) was dissolved in 5 ml of CHCl₃ and TFB (0.313 g, 1.93 mmol) dissolved in 5 ml CHCl₃ and trifluoroacetic acid (0.056 ml, 0.72 mmol) were added. After heating the reaction mixture at 60°C for 72 hrs, the solvent was removed under reduced pressure and the crude purified by column chromatography (9:1, benzene: ethyl acetate) to give a yellow waxy solid 0.57 g (54 % yield).

M.p. = 50°C.

¹H-NMR (300 MHz, CDCl₃): δ 8.01 (s, 12H), 7.95 (s, 12H), 3.32 (d, ³J_{HH} = 9Hz, 12H), 1.76-1.61 (m, 24 H), 1.21 (m, 144 H), 0.83 (t, ³J_{HH} = 8 Hz, 36 H).

¹³C-NMR (125 MHz, CDCl₃): δ 159.7, 137.0, 129.9, 75.8, 32.3, 32.2, 29.9, 29.8, 26.7, 23.0, 14.4.

MS (MALDI-TOF⁺) 2139 ([M+H]).

CHN analysis for C₁₄₄H₂₄₀N₁₂: C 80.84, H 11.31, N 7.86; found C 80.84, H 10.60, N 7.88.

Formation of fibres of octyl cage (9)

A sample of octyl cage (9) (100 mg) in a small round-bottomed flask was heated to 100°C to form a viscous liquid. The tip of a Pasteur pipette was inserted into the liquid and withdrawn ca. 0.2 m at ca. 2 ms⁻¹ to produce a 0.2 m fibre.

^1H and ^{13}C NMR of compound 6, 7,8,9.

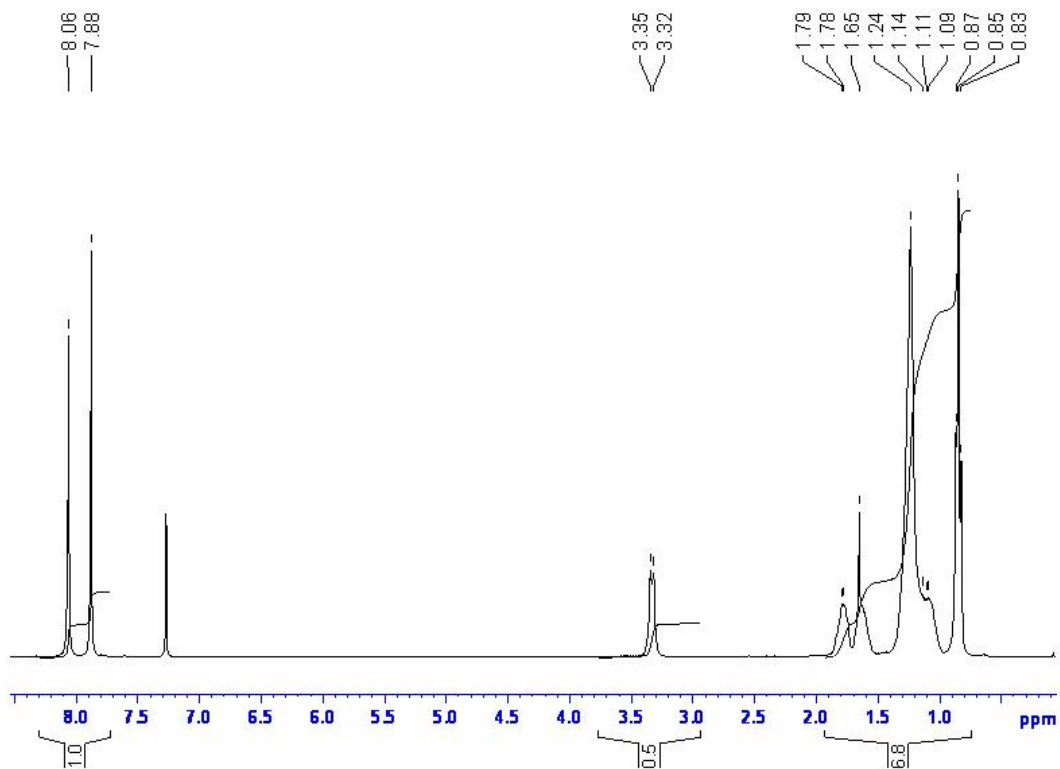


Figure S2. ^1H -NMR (300 MHz, CDCl_3) of the hexyl cage (**6**).

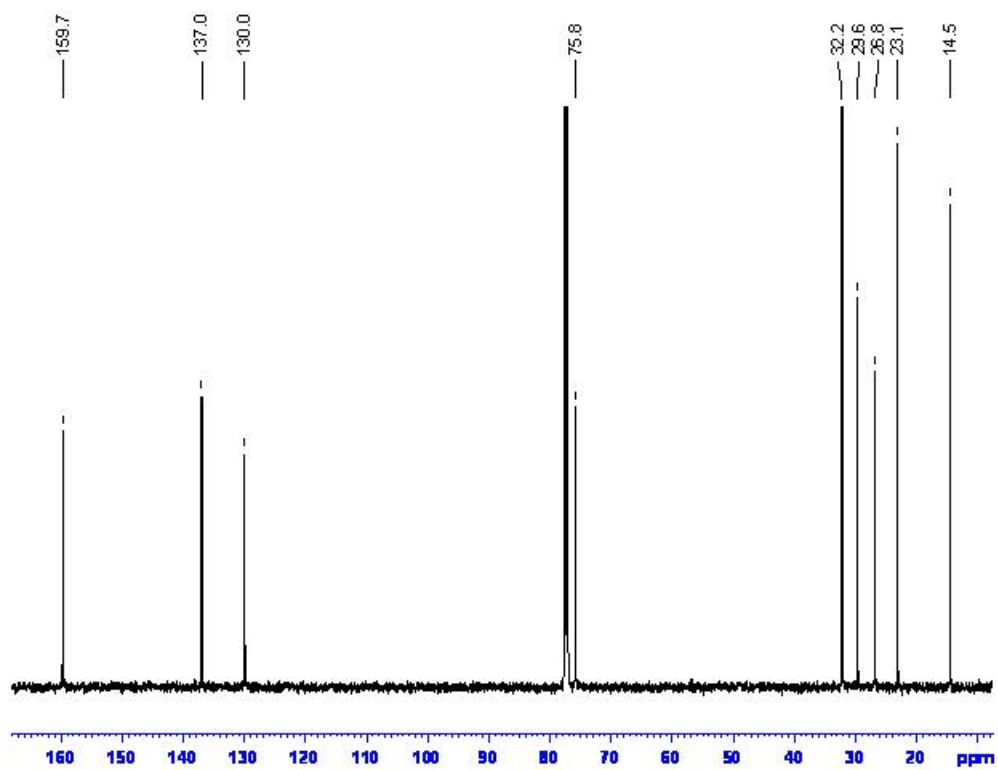


Figure S2. ^{13}C -NMR (125 MHz, CDCl_3) of the hexyl cage (6).

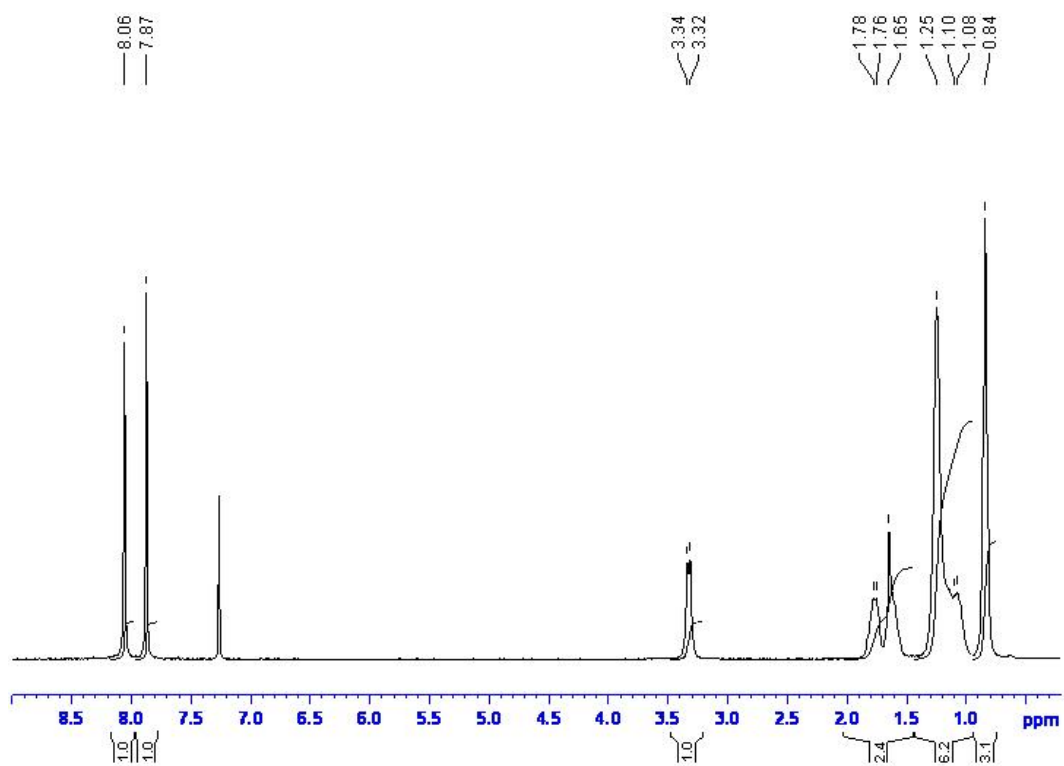


Figure S3. ^1H -NMR (300MHz, CDCl_3) of the pentyl cage (7).

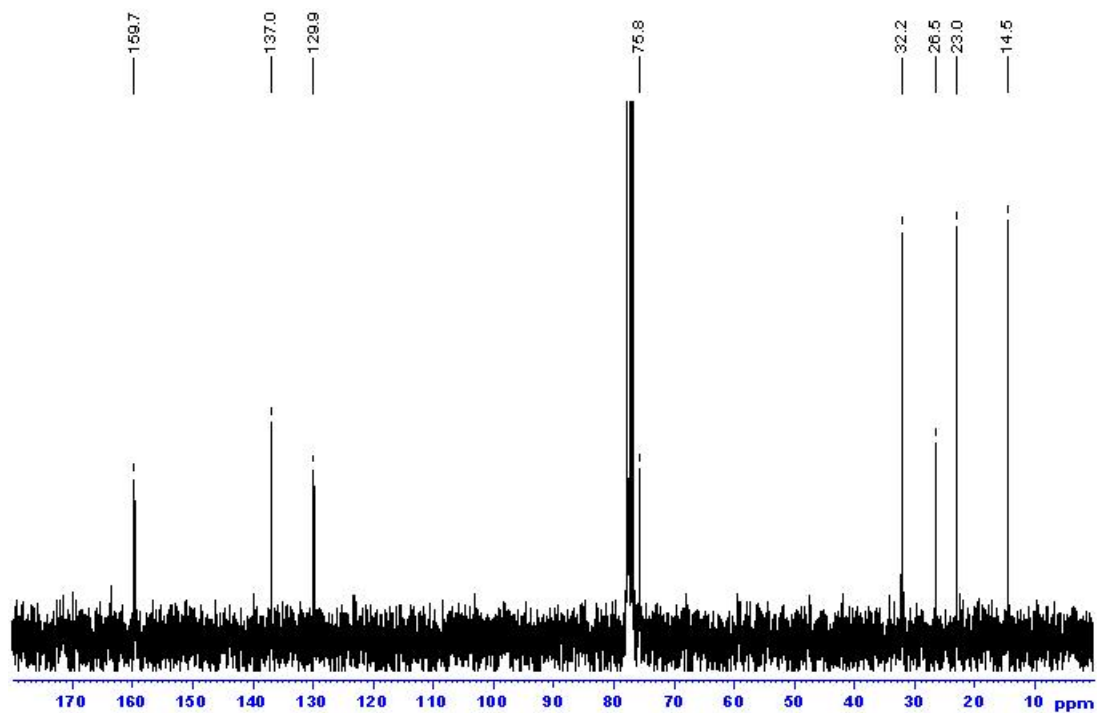


Figure S4. ^{13}C -NMR (75 MHz, CDCl_3) of the pentyl cage (7).

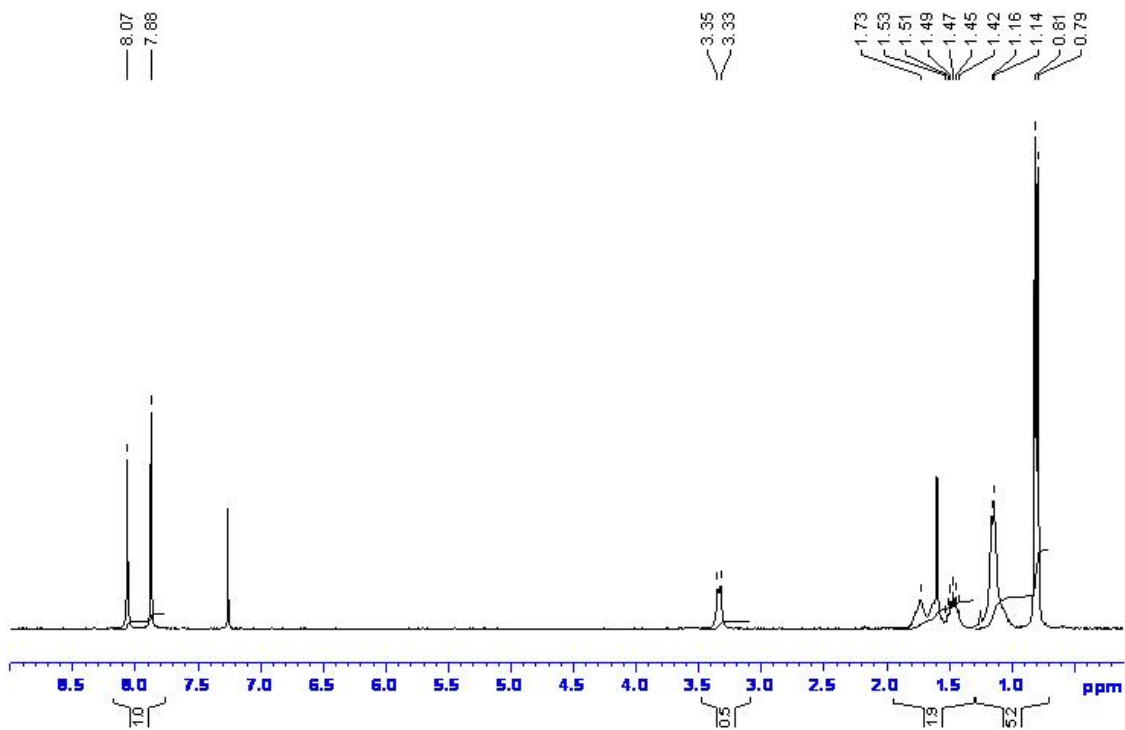


Figure S5. ^1H -NMR (300 MHz, CDCl_3) of the isohexyl cage (8).

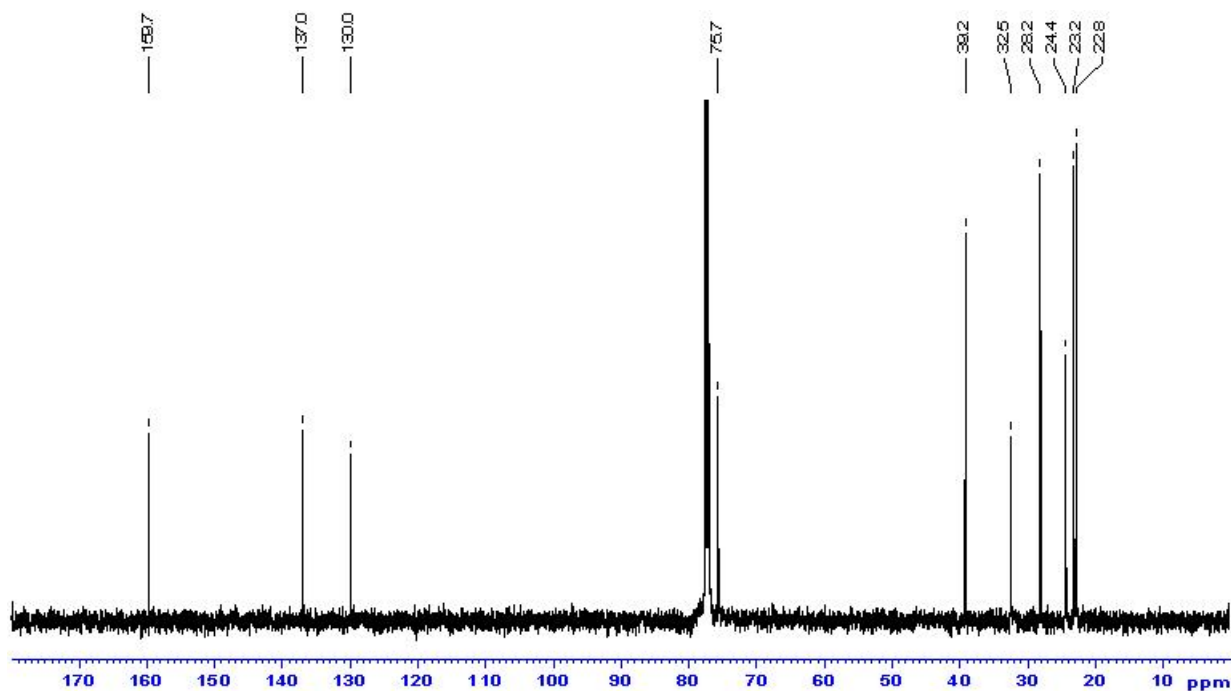


Figure S6. ^{13}C -NMR (125 MHz, CDCl_3) of the isohexyl cage (8).

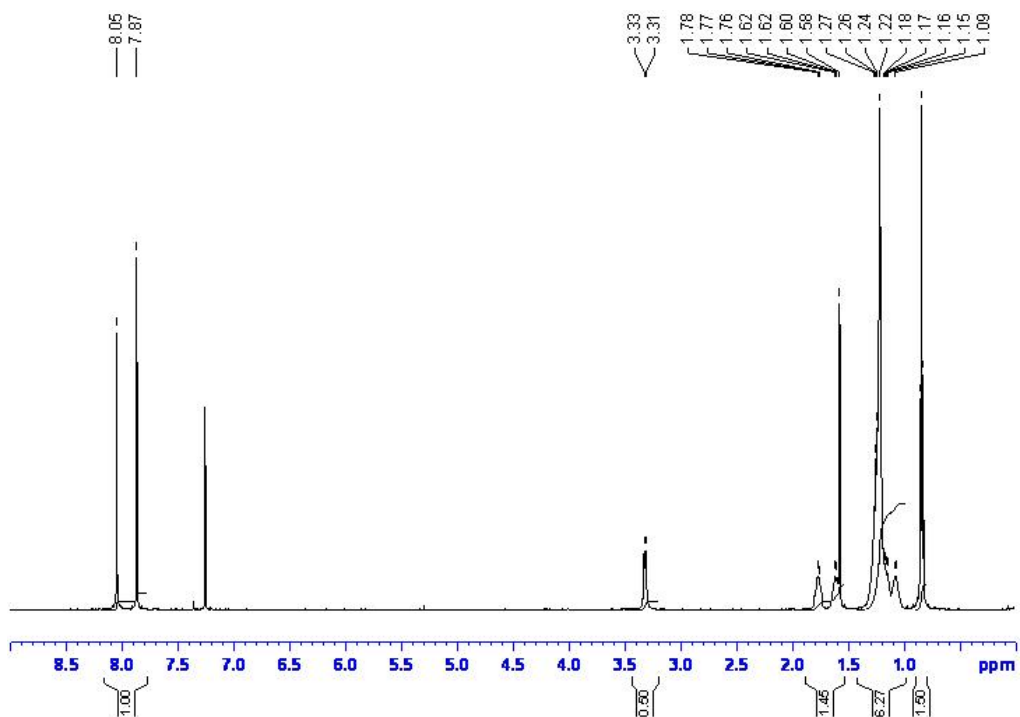


Figure S7. ^1H -NMR (300 MHz, CDCl_3) of the octyl cage (9).

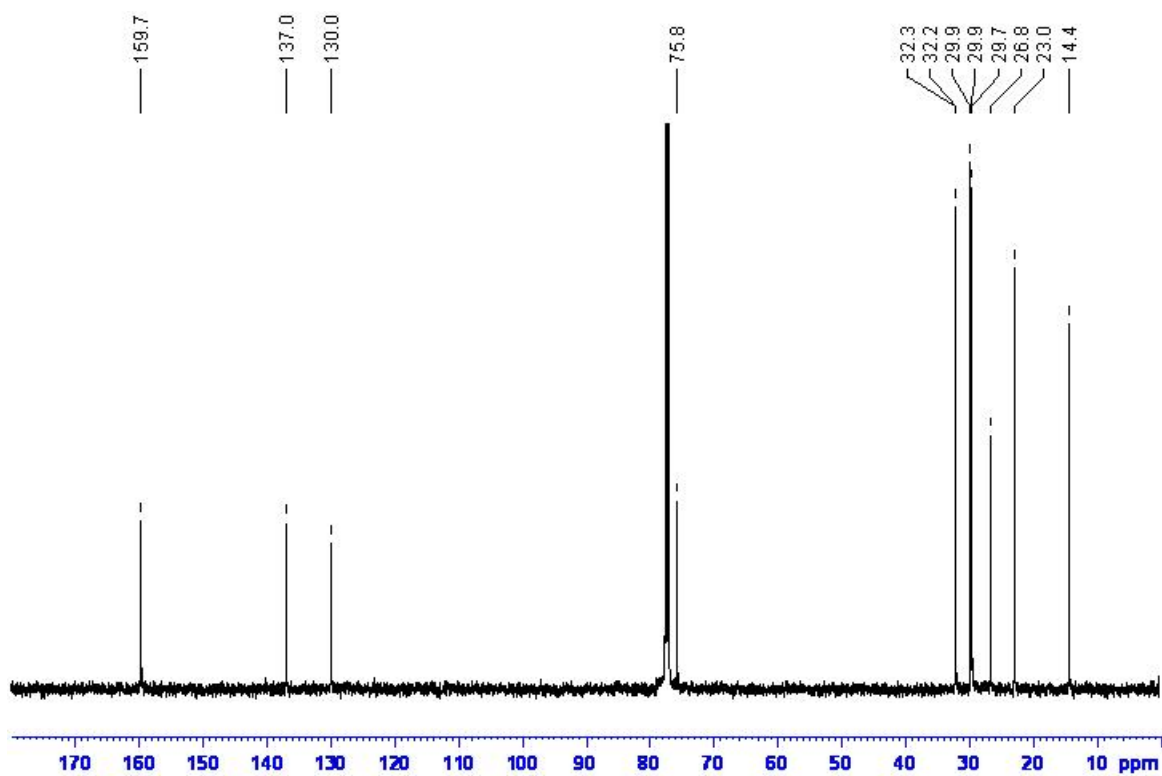


Figure S8. ^{13}C -NMR (125 MHz, CDCl_3) of the octyl cage (8).

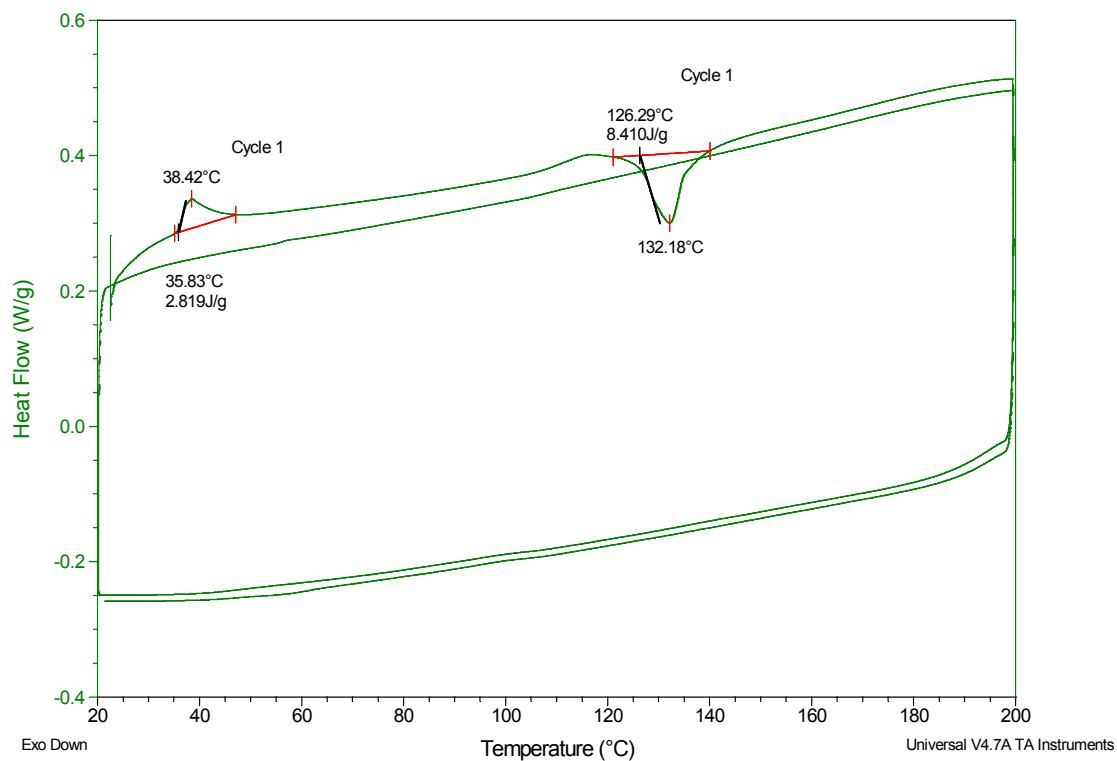


Figure S9. DSC trace of the hexyl cage (6) (two heating-cooling cycles performed)

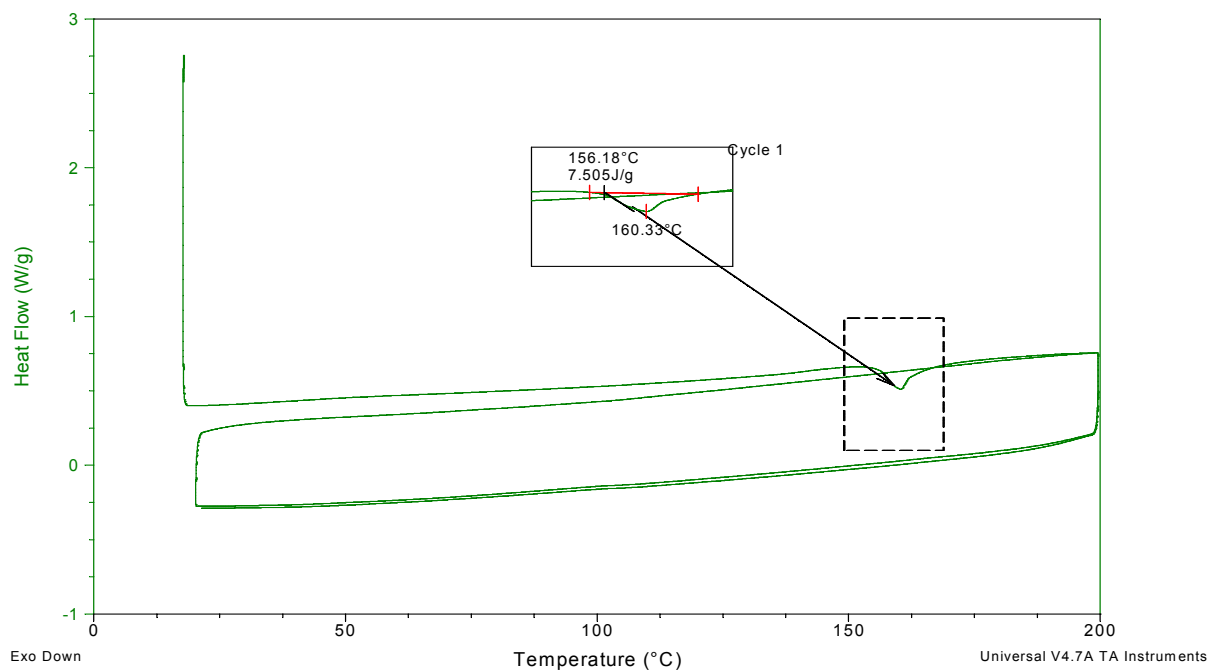


Figure S10. DSC trace of the pentyl cage (7) (two heating-cooling cycles performed)

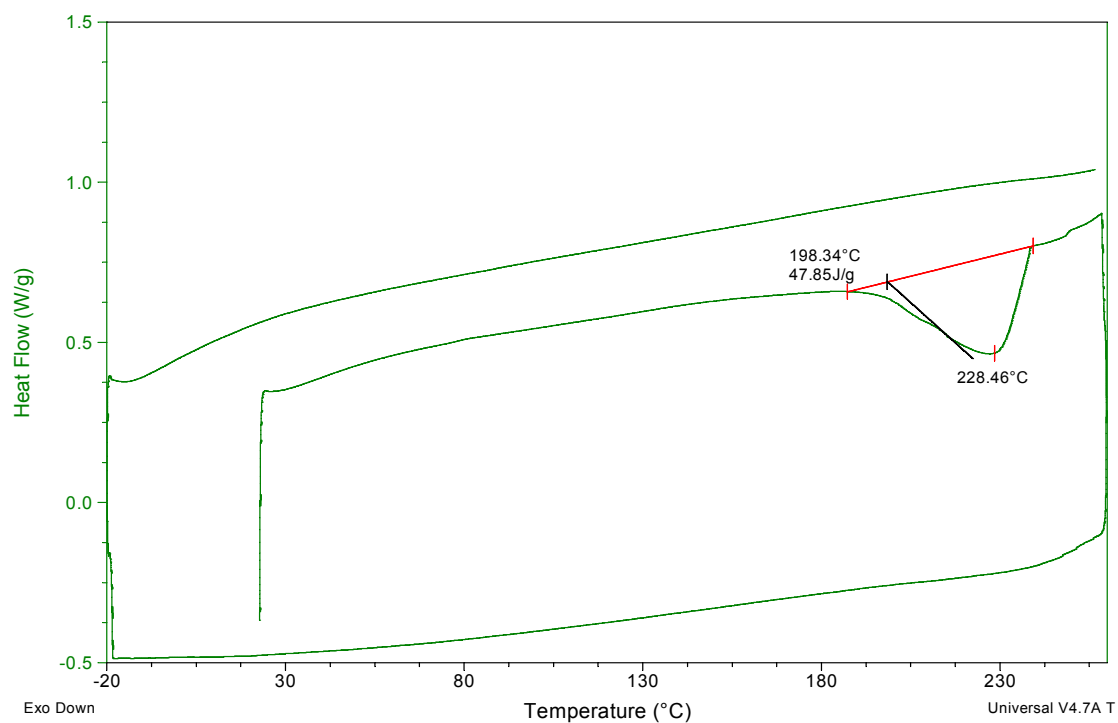


Figure S11. DSC trace of the isohexyl cage (**8**) (two heating-cooling cycles performed)

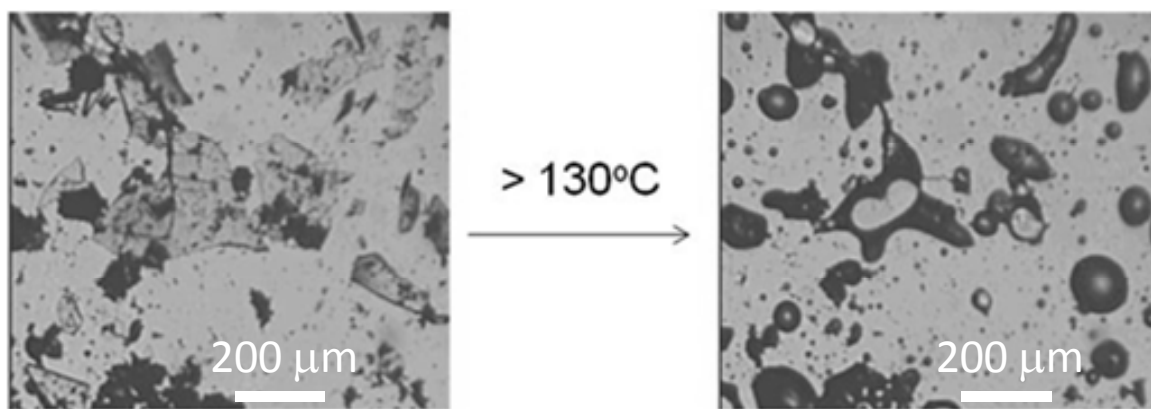


Figure S12. Visual melting of the hexyl cage (**6**).

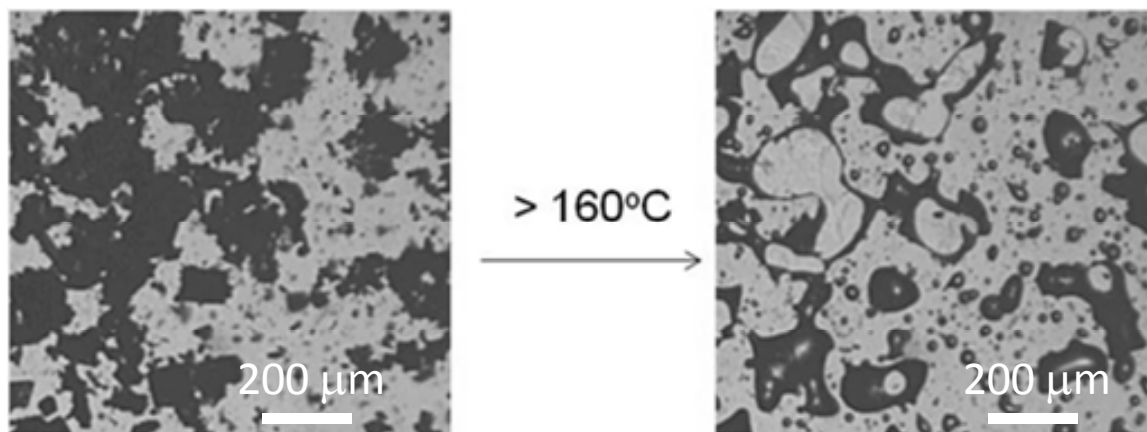


Figure S13. Visual melting of the pentyl cage (**7**).

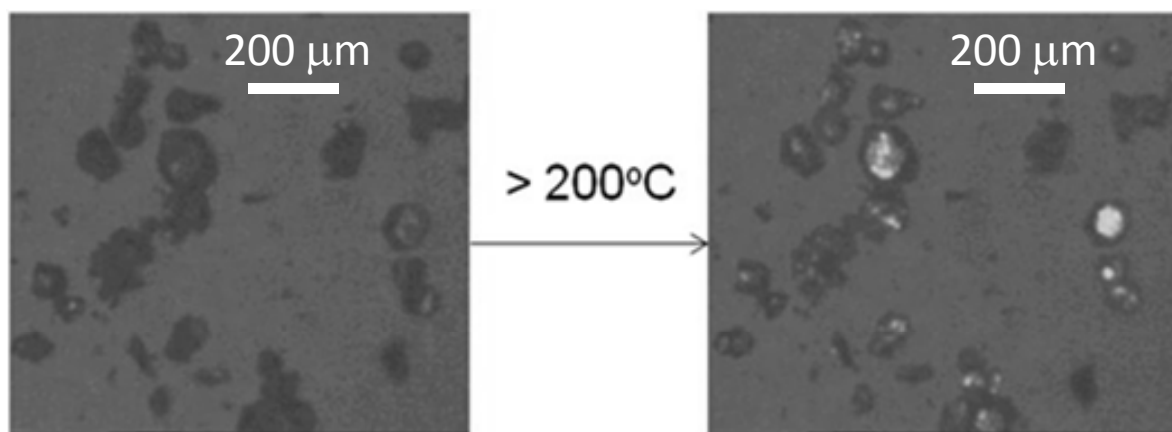


Figure S14. Visual melting of the isohexyl cage (**8**).

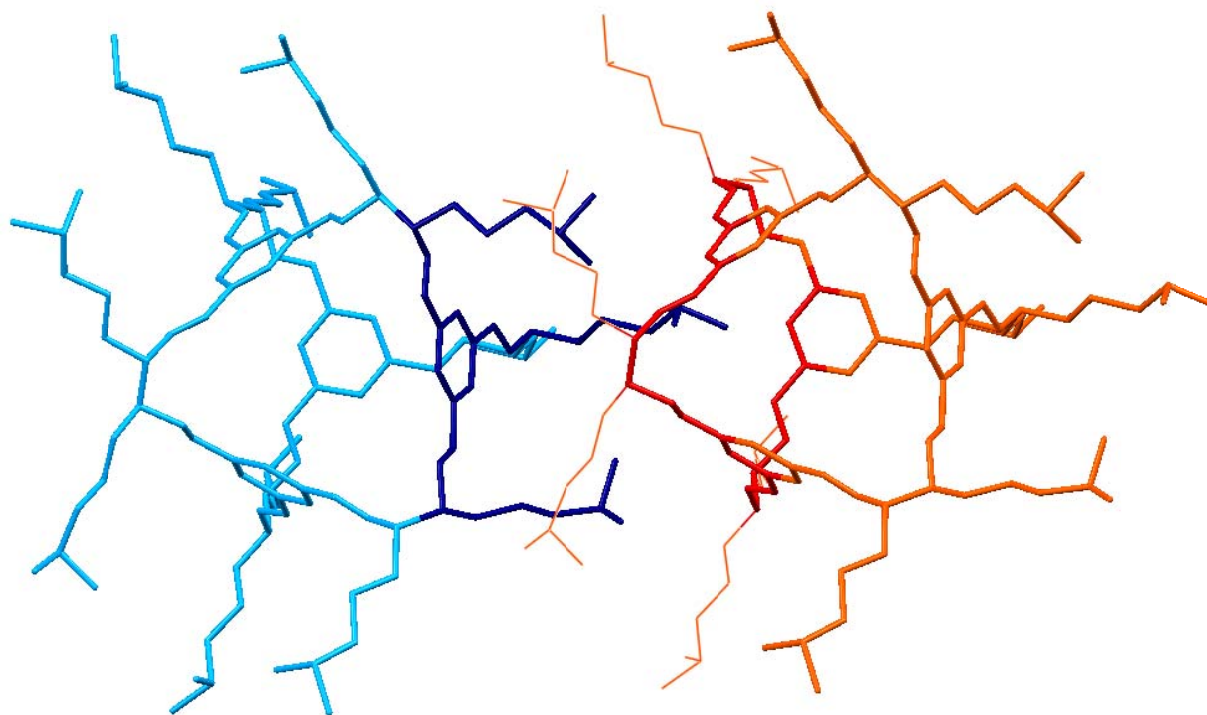


Figure S15 The packing motif in the crystal structure of isohexyl cage **8** (H-atoms and solvent molecules omitted for clarity).

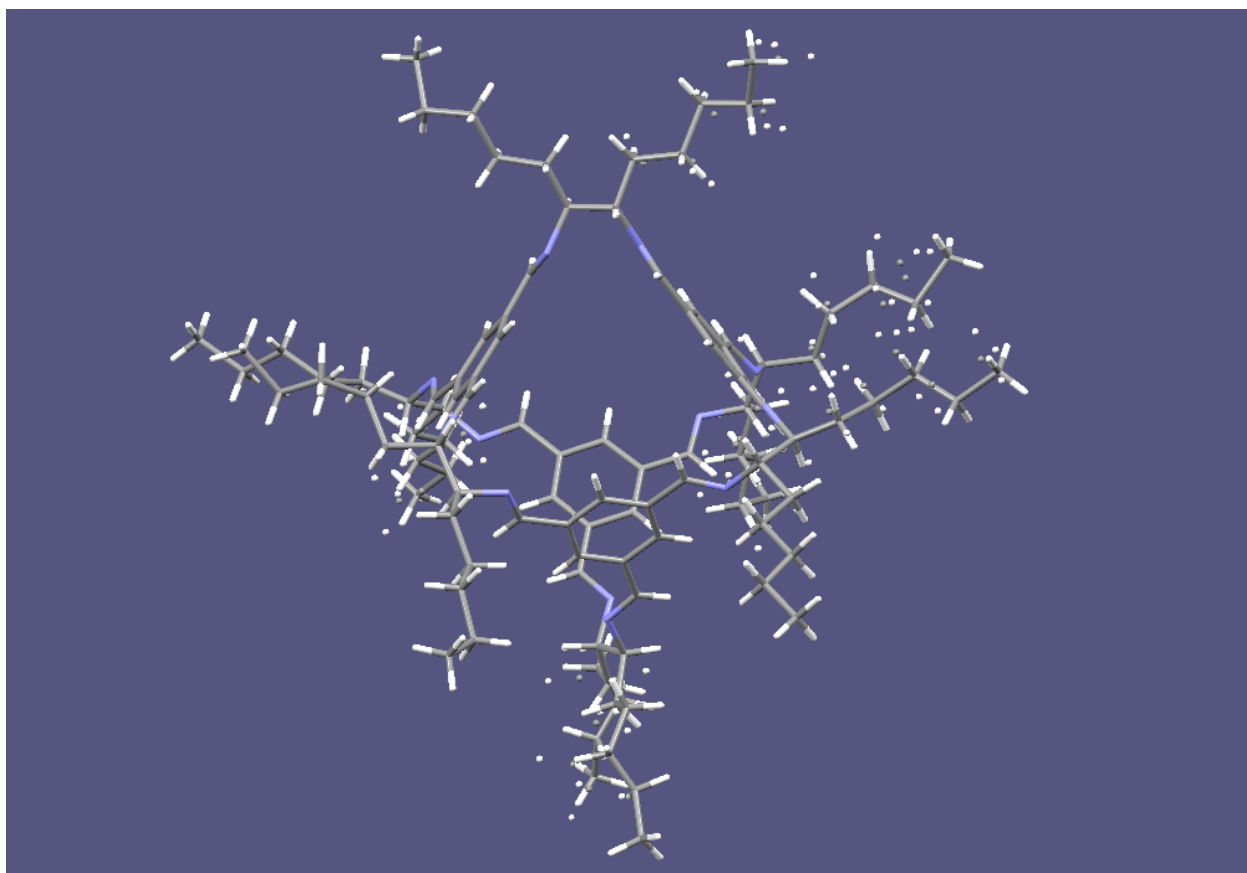


Figure S16 Molecular structure of *n*-pentyl cage **7** in the crystal showing the disorder in the chains (solvent molecules omitted for clarity).

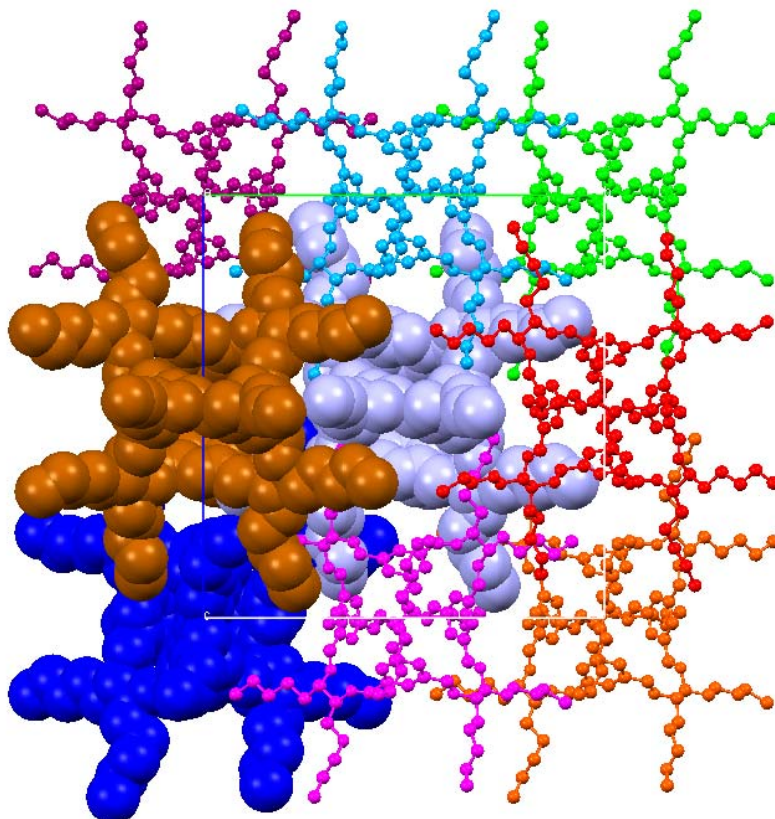


Figure S17 View of the crystal structure of *n*-pentyl cage 7 along the crystallographic *a* axis (H-atoms and solvent molecules omitted for clarity).

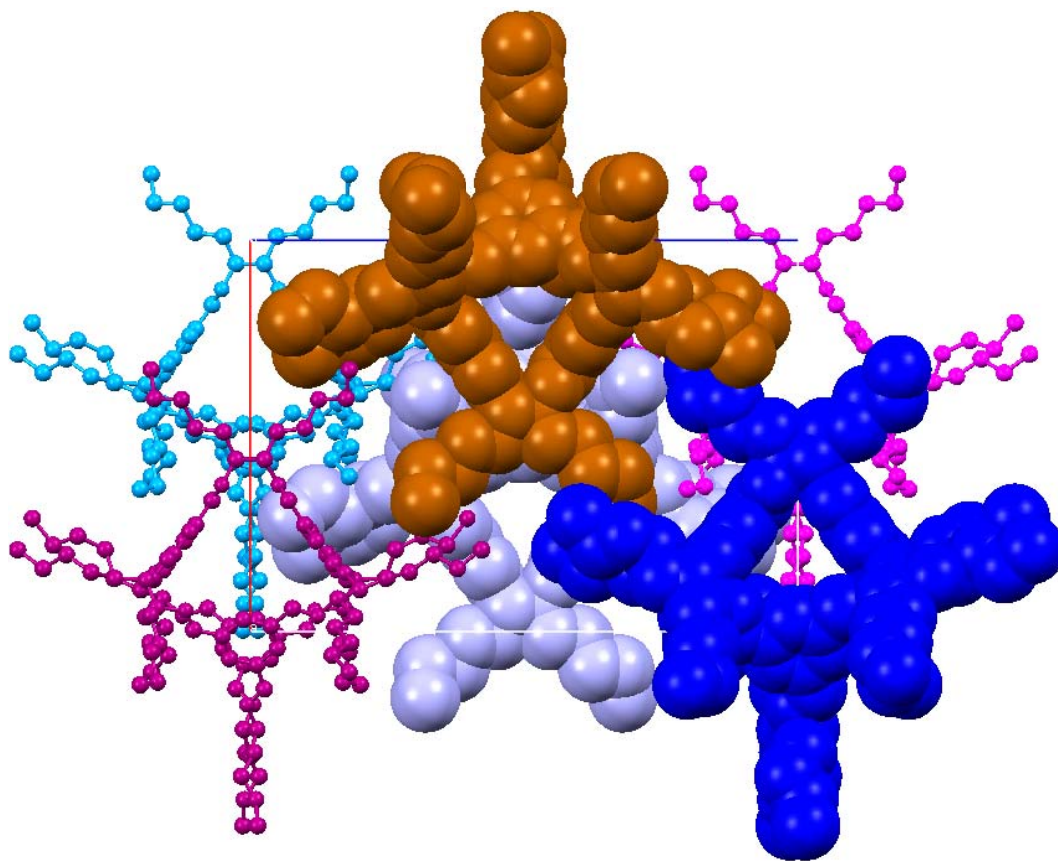


Figure S18 View of the crystal structure of *n*-pentyl cage 7 along the crystallographic *b* axis (H-atoms and solvent molecules omitted for clarity).

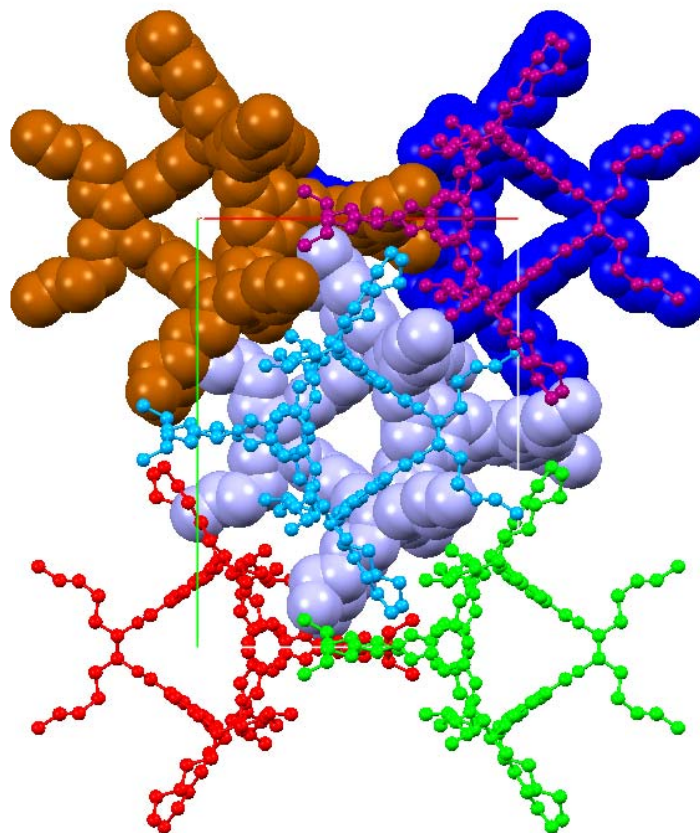


Figure S19 View of the crystal structure of *n*-pentyl cage 7 along the crystallographic *c* axis (H-atoms and solvent molecules omitted for clarity).

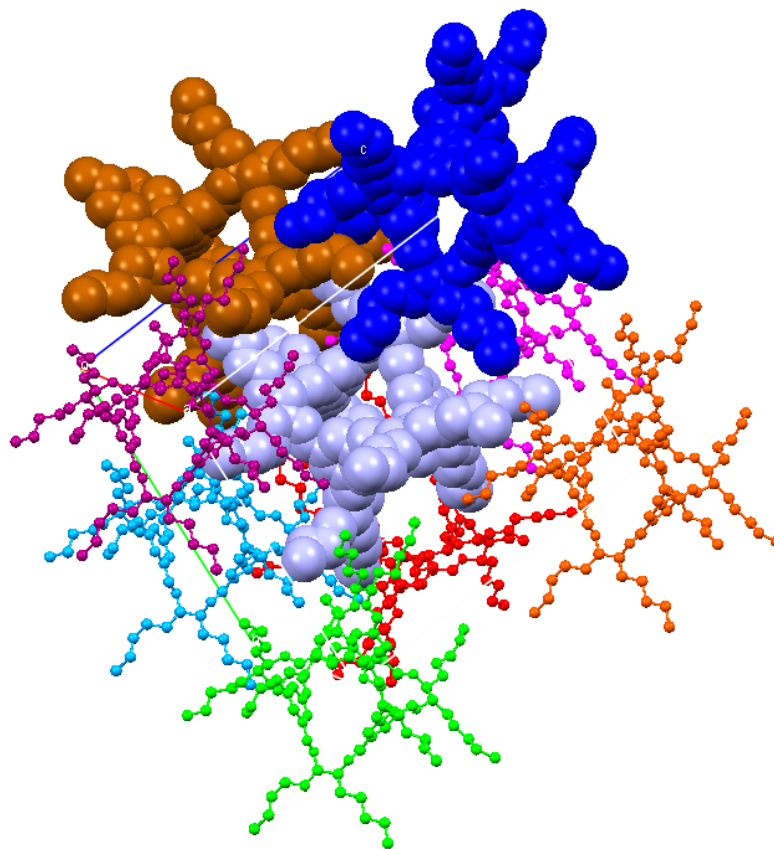


Figure S20 View of the crystal structure of *n*-pentyl cage 7 between the crystallographic axes (H-atoms and solvent molecules omitted for clarity).

Rheology study

All testing was conducted on a Malvern Kinexus rotational rheometer with peltier plate temperature control, conducted on a 8mm plate with 8mm pedestal plate. A 0.5mm gap was used as this is considered the minimum plausible gap for the high modulus in the temperature range used. The sample volume when molten was ≈ 0.1 ml.

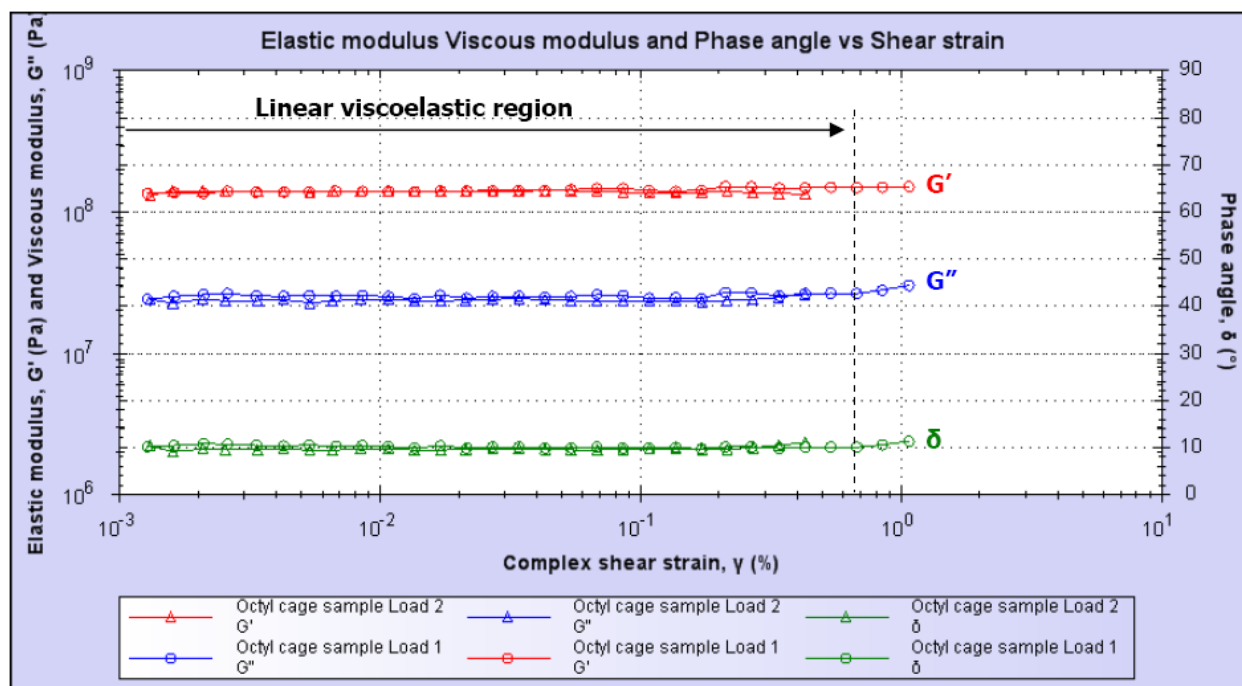


Figure S21. Amplitude sweep for the cage 9 showing Elastic modulus G' (Pa), Viscous modulus G'' (Pa) and phase angle δ ($^\circ$) with increasing strain γ (%). 50°C, 1Hz. Load 1 (circles) and Load 2 (triangles).

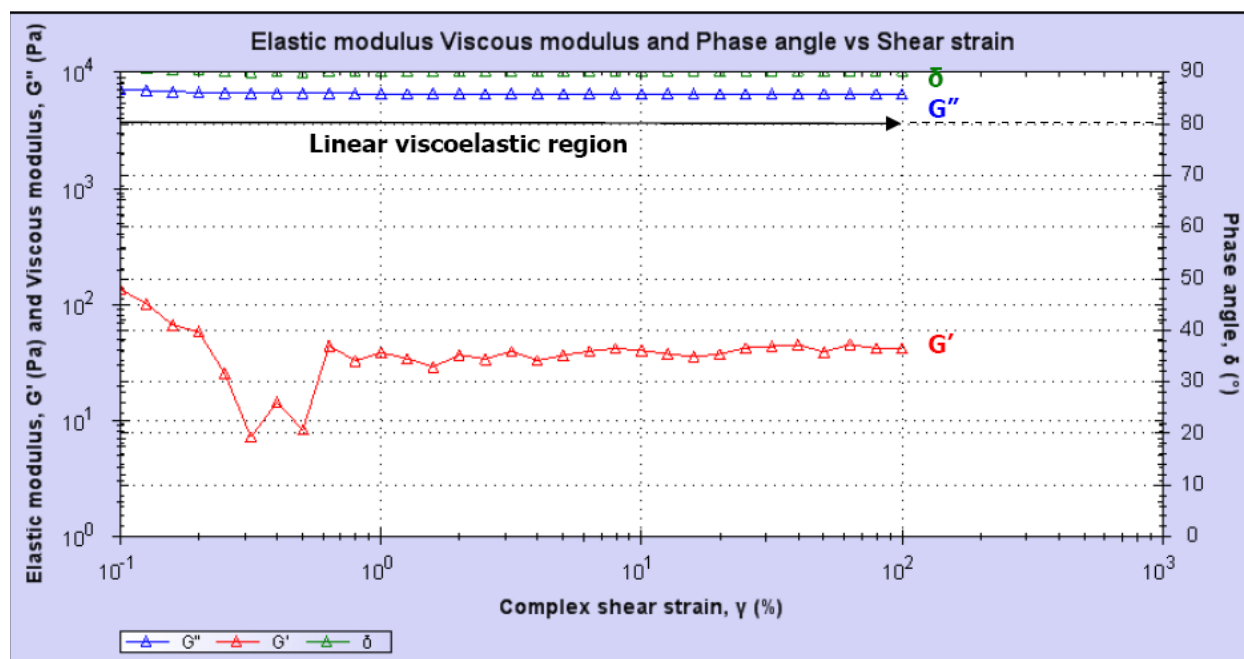


Figure S22. Amplitude sweep for cage **9** showing Elastic modulus G' (Pa), Viscous modulus G'' (Pa) and phase angle δ ($^\circ$) with increasing strain γ (%). 100°C , 1Hz.

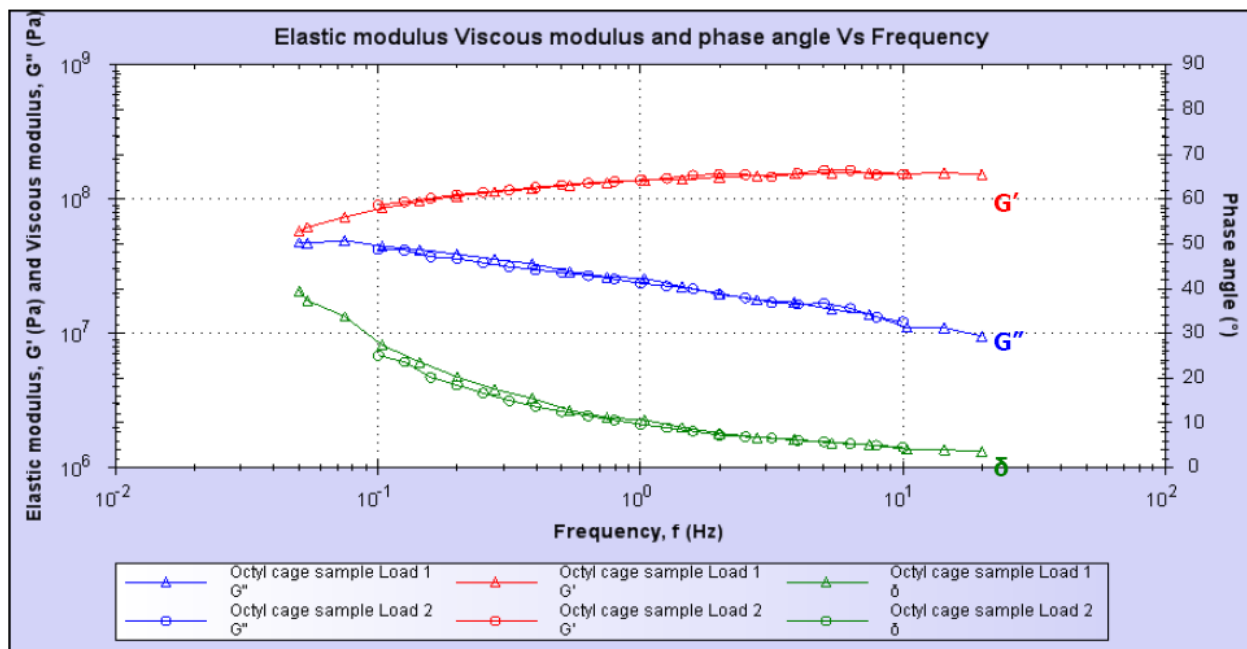


Figure S23. Frequency sweep for cage 9 showing Elastic modulus G' (Pa), Viscous modulus G'' (Pa) and phase angle δ ($^\circ$) across a range of frequencies at 50°C . Load 1 (triangles) and Load 2 (circles)

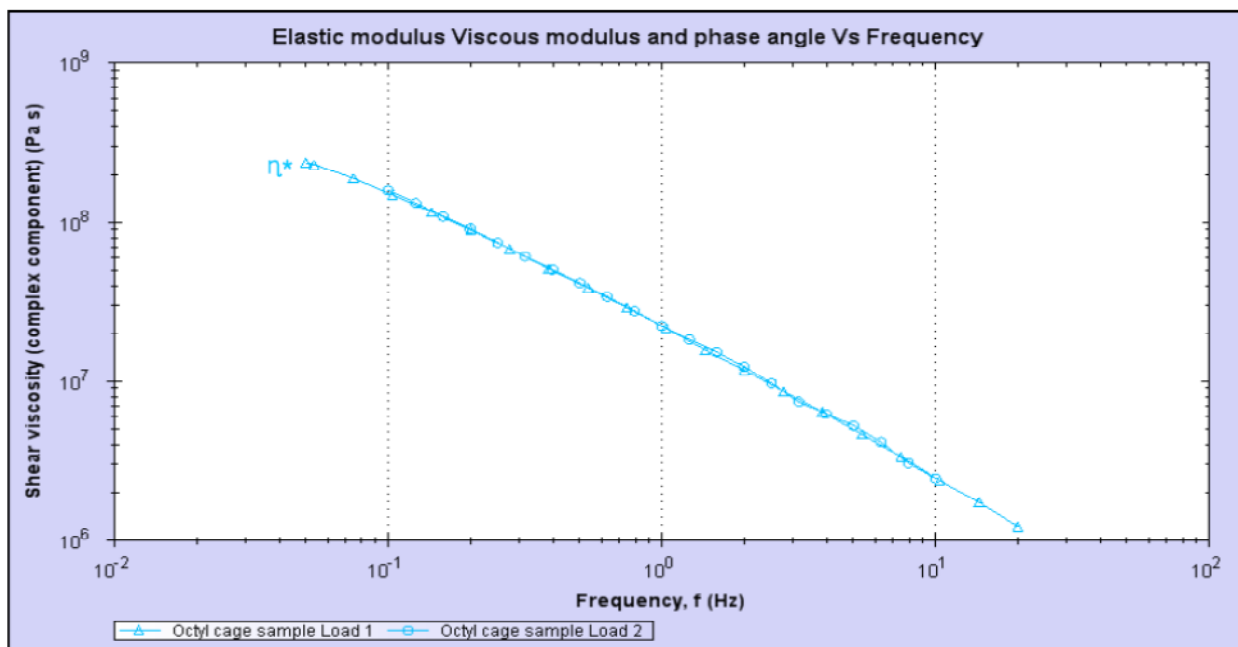


Figure S24. Frequency sweep for cage 9 showing Complex viscosity η^* (Pa.s) across a range of frequencies at 25°C. Load 1 (triangles) and Load 2 (circles).

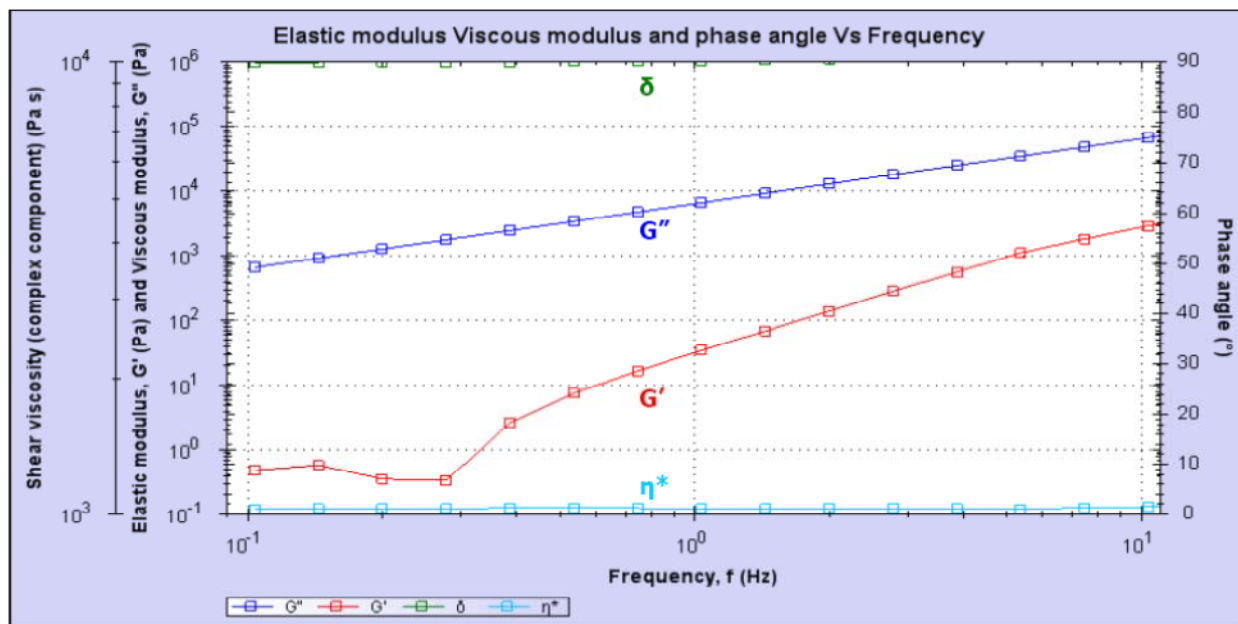


Figure S25. Frequency sweep for cage 9 showing elastic modulus G' (Pa), viscous modulus G'' (Pa), complex viscosity η^* (Pa.s) and phase angle δ (°) across a range of frequencies at 100°C.

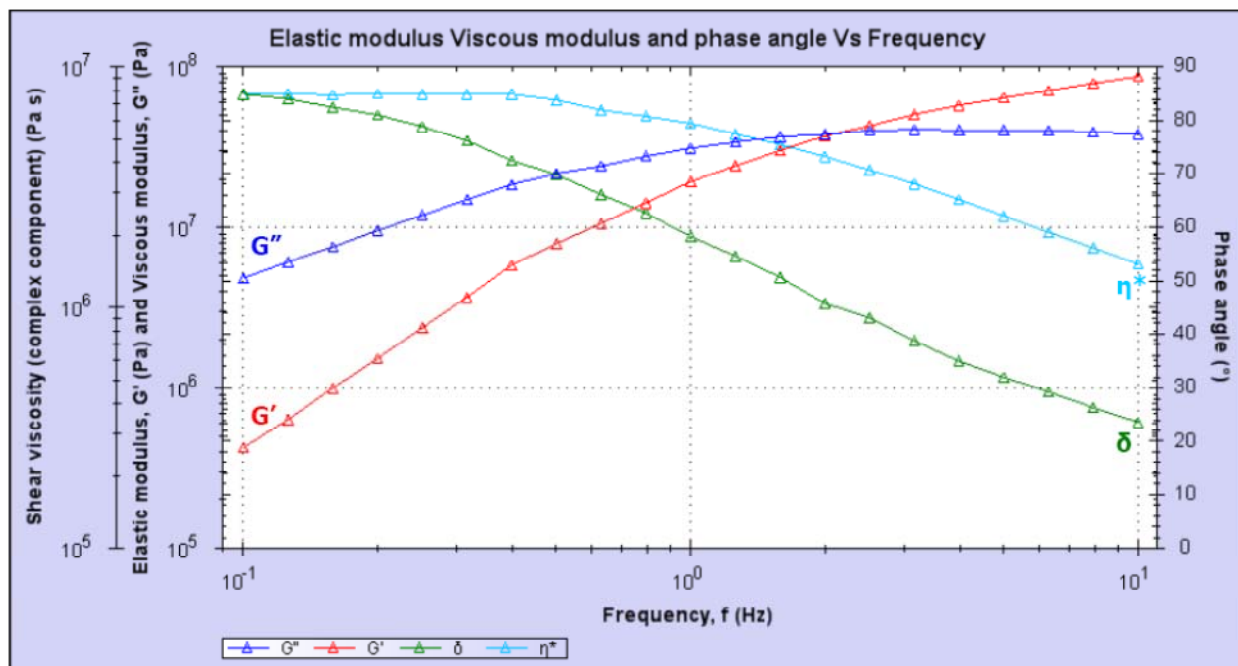


Figure S26. Frequency sweep for cage 9 showing elastic modulus G' (Pa), viscous modulus G'' (Pa), complex viscosity η^* (Pa.s) and phase angle δ ($^\circ$) across a range of frequencies at 60°C.

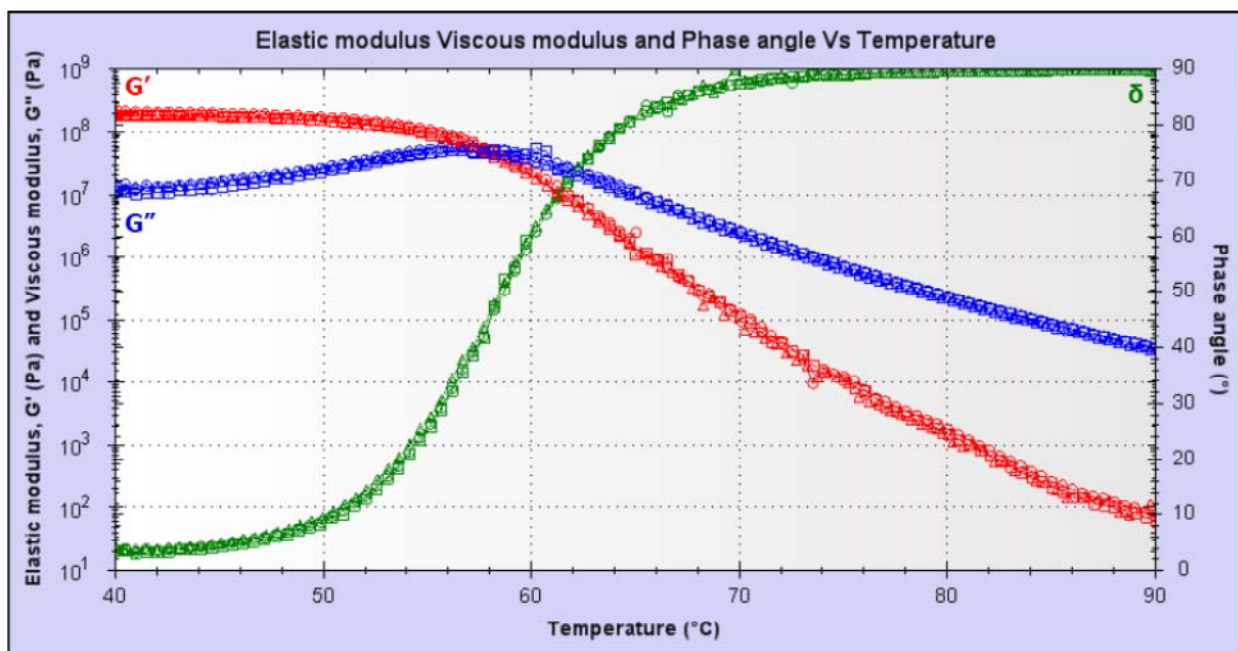


Figure S27. Temperature sweep of cage **9** between 40°C and 90°C, at 1Hz and 2°C/min showing showing Elastic modulus G' (Pa), viscous modulus G'' (Pa) and phase angle δ (°). Load 1 (triangles), Load 1.2 (squares) and Load 2 (circles).

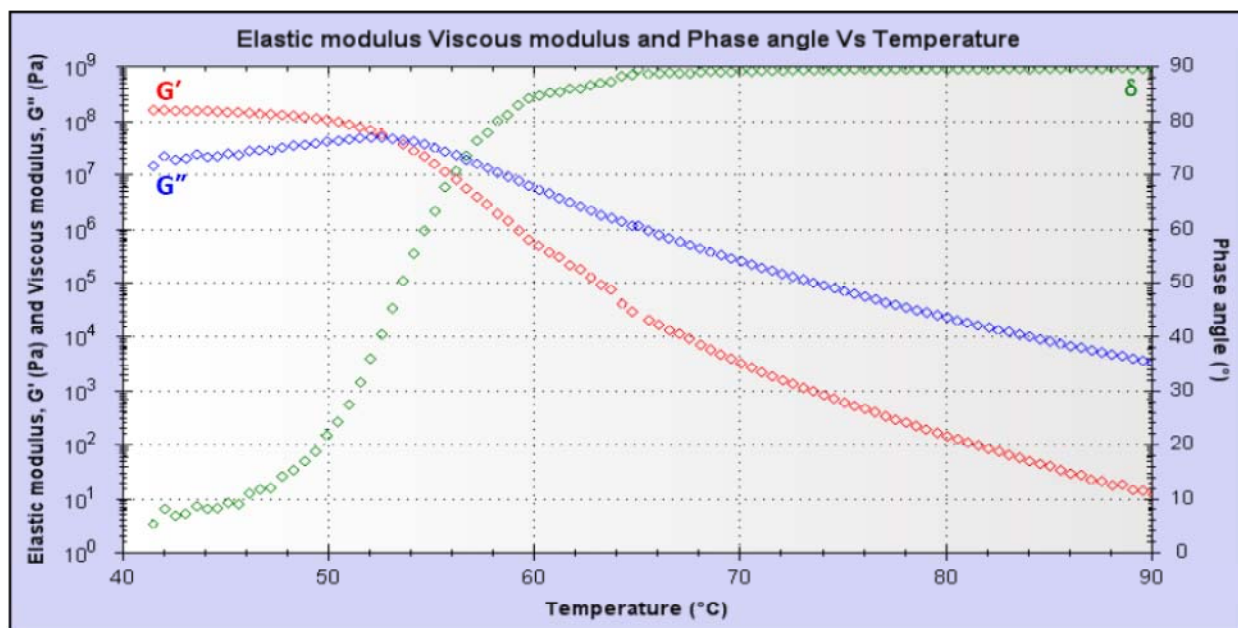


Figure S28. Temperature sweep of cage **9** between 40°C and 90°C, at 0.1Hz and 2°C/min showing elastic modulus G' (Pa), viscous modulus G'' (Pa) and phase angle δ (°). Load 1.1(0.1Hz).

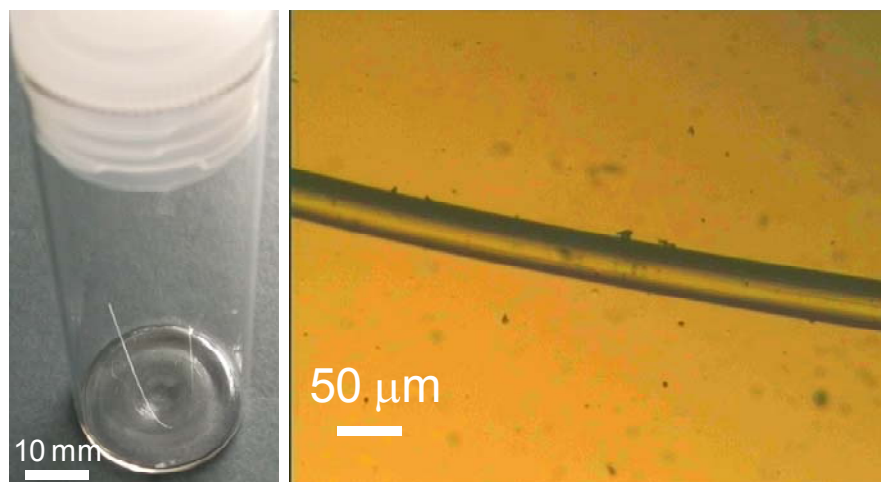


Figure S29. Photographs of a fibre of cage **9** drawn out from the melt.

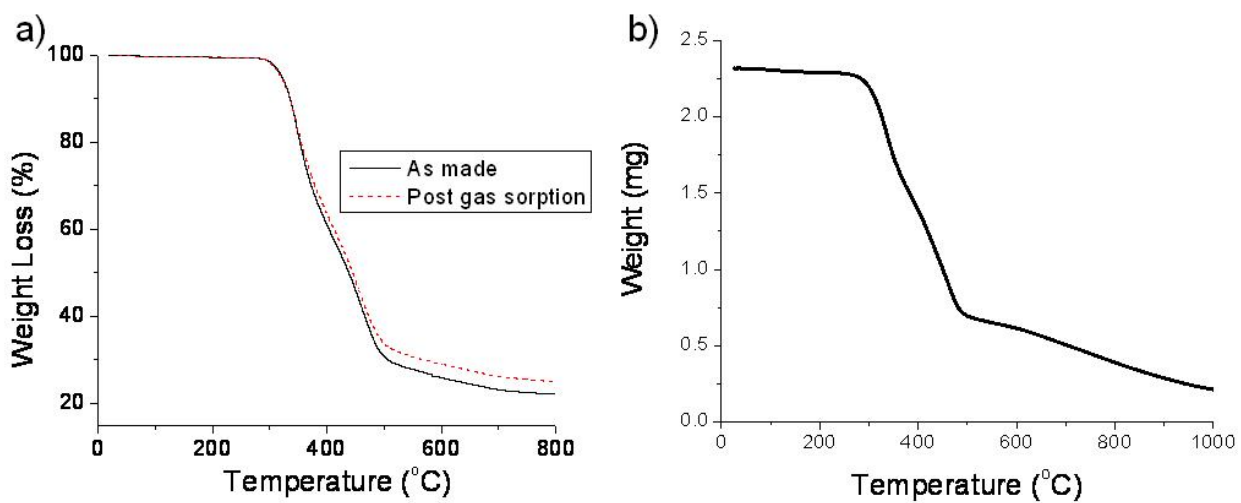


Figure S30. a) TGA of the isohexyl cage **8**, b) TGA of the octyl cage **9**.

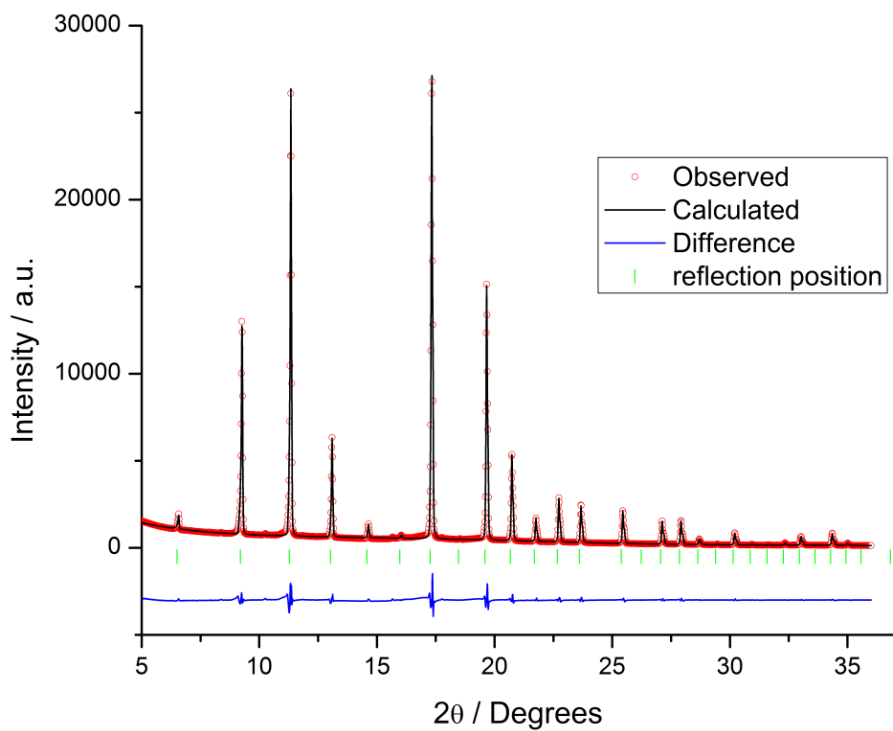


Figure S31. PXR Le Bail profile fit of the desolvated isohexyl cage **8** measured after gas sorption analysis. (space group $I23$, $a = 19.2015(6)$ Å, $V = 7079(6)$ Å³, Agreement factors, $R_{wp} = 6.36$, $R_{exp} = 3.55$, $R_p = 4.50$, $GoF = 1.79$).

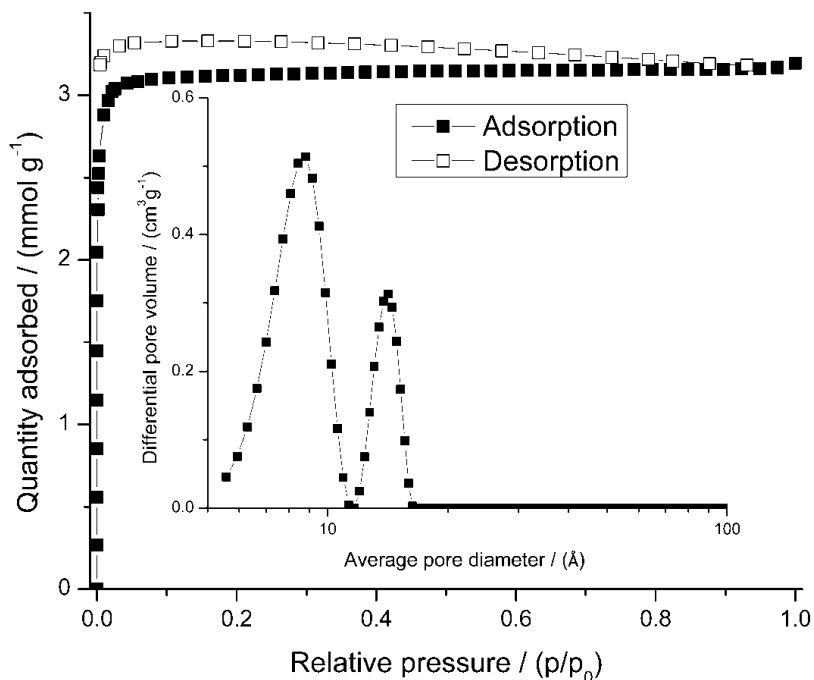


Figure S32. N₂ adsorption/ desorption isotherm recorded at 77 K on the isohexyl cage **8**. Inset is the NL-DFT pore size distribution plot calculated using the adsorption branch of the isotherm.

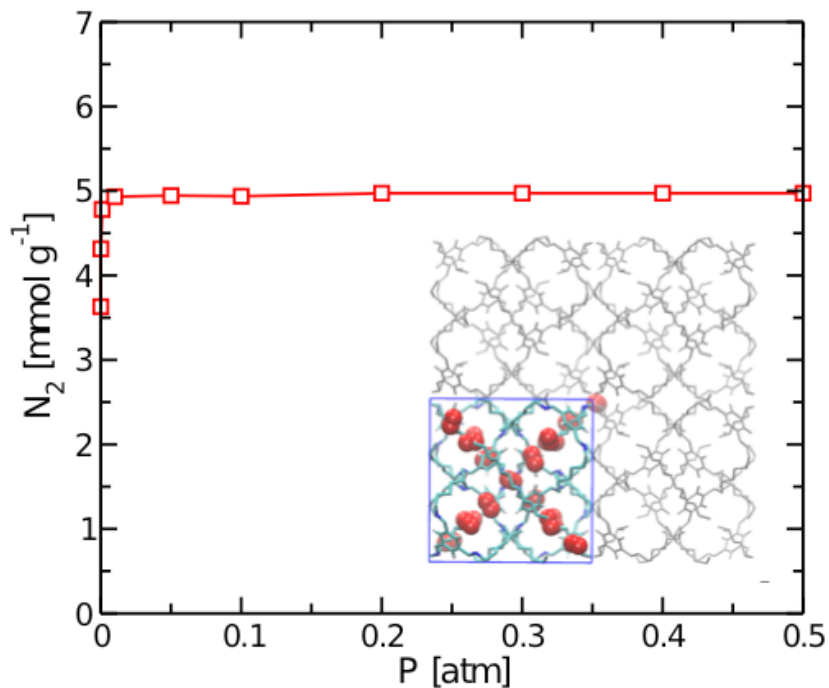


Figure S33. Simulated N₂ absorption isotherm at 77 K. Inset: snapshot of the fully saturated system. N₂ molecules outside the marked unit cell have been removed. The maximum uptake of 5 mmol g⁻¹ corresponds to nine N₂ molecules per cage.

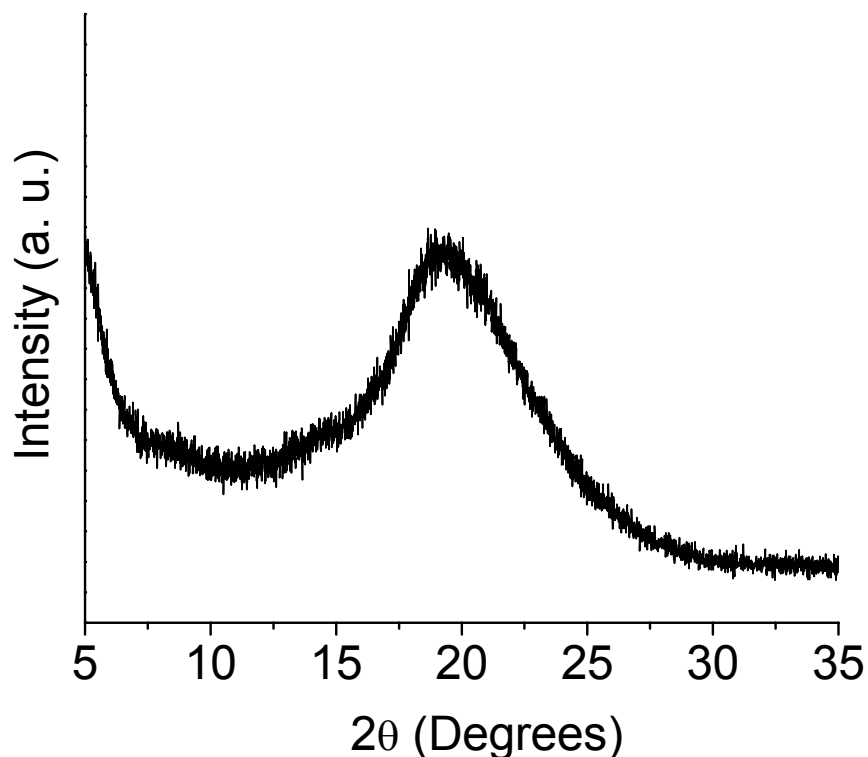


Figure S34. Powder X-ray diffraction pattern for octyl cage **9**.

1. R. Hoof, *Collect, Data collection software*, Nonius BV, Delft, The Netherlands, 1998.
2. Z. Otwinowski and W. Minor, *Methods Enzymol.*, 1997, **276**, 307–326.
3. G. M. Sheldrick, *SADABS, Program for area detector adsorption correction*, Institute for Inorganic Chemistry, University of Göttingen, Germany, 1996
4. G. M. Sheldrick, *Acta Crystallogr. A*, 2008, **64**, 112
5. P. v.d. Sluis and A. L. Spek, *Acta Crystallogr., A*, 1990, **46**, 194-201.
6. A.L. Spek, (2003). *J. Appl. Cryst.* 36, 7-13.
7. W.J. Jorgensen and Tirado-Rives, *J. Proc. Nat. Acad. Sci, USA*, 2005, **102**, 6665—6670.
8. A.L. Galbraith and C.K. Hall, *Fluid Phase Equilibria*, 2006, **241**, 175—185.
9. S. M. Dimick, S. C. Powell, S. A. McMahon, D. N. Moothoo, J. H. Maismith and E. J. Toone, *J. Am. Chem. Soc.*, 1999, **121**, 10296-10296.
10. N. Kaur, J. G. Delcros, J. Imran, A. Khaled, M. Chehtane, N. Tschammer, B. Martin and O. Phanstiel, *J. Med. Chem.*, 2008, **51**, 1393-1401.